Saint Petersburg State University

Ilya Alekseev

Graduation qualification thesis

New classes of minimal knot diagrams

Bachelor's program
"Mathematics"
Specialization and code: 01.03.01 "Mathematics"
Cipher of the EP: SV.5000.2016

Thesis supervisor:
Senior research fellow,
PDMI,
Doctor of Science,
Andrei V. Malyutin

Thesis reviewer:
Leading researcher,
University of Geneva,
Laboratory "Modern
Algebra and Applications",
Professor,
Tatiana V. Smirnova-Nagnibeda

Saint Petersburg
2020

Abstract

The present thesis is devoted to knot theory. We study diagrams of knots, links, braids, and tangles with the minimum number of crossings, the minimum number of Seifert circles, and other properties. One of the main results is the construction of a new class of link diagrams with the minimum number of crossings. This class includes many alternating diagrams, torus ones, and numerous diagrams whose minimality has not been proven before. Besides, we construct a new larger class of link diagrams with the minimum number of Seifert circles. Also, we provide results related to geometric group theory. In particular, we describe simple criteria on a braid diagram representing a conjugacy class of a homogeneous braid to have the minimum number of crossings.

Contents

1. Introduction

We use basic terminology and notions of knot theory as introduced in [3].

The central notions of the present thesis are minimal link diagrams and the crossing number of links. The latter is a natural complexity measure of links. Recall that a diagram $\mathcal{D}$ of a link $\mathcal{L}$ is said to be *minimal* if $\mathcal{D}$ has the least number of crossings among all diagrams of $\mathcal{L}$. The number of crossings of a minimal diagram of $\mathcal{L}$ is called the *crossing number* of $\mathcal{L}$.

Historically, the crossing number is closely related to the recognition problem for links. This problem is one of the most fundamental questions of both the early stages of knot theory and nowadays. The recognition problem requires to construct an algorithm that decides whether two given diagrams represent the same link. Given such an algorithm, one could determine whether a diagram $\mathcal{D}$ having n crossings is minimal as follows. List all diagrams $\mathcal{U}$ with less than n crossings, and for each $\mathcal{U}$, determine whether $\mathcal{U}$ and $\mathcal{D}$ represent the same link.

In theory, the link recognition problem has been solved (see an expository note [20]). The main work, which is based on the theory of normal surfaces, was done by W. Haken, F. Waldhausen, and K. Johannson, with important contributions by S. V. Matveev, G. Hemion, W. Jaco, and P. B. Shalen. Still, the corresponding algorithm is impractical due to complexity issues. On the other hand, for certain classes of links, spectacular classification results have been obtained. The examples include torus links, rational links, braid index 3 links,

alternating links, and hyperbolic links (see [4]). The last two classes have proven especially useful to a link tabulator wanting to classify all links up to a given crossing number.

At the same time, several remarkable phenomena were discovered concerning minimal diagrams. Namely, some easy to verify visual properties of link diagrams guarantee the minimality. The examples include reduced alternating diagrams, adequate diagrams, reduced Montesinos diagrams, and closed GMM braid diagrams, which we describe below.

One of the main results of the present thesis is the construction of a new class of minimal link diagrams of this kind.

Let us describe the known classes of minimal link diagrams and their role in the development of knot theory in more detail.

Recall that a link diagram $\mathcal{D}$ is said to be *alternating* if, as one follows each link component of $\mathcal{D}$, one passes overcrossings and undercrossings alternatively. A link $\mathcal{L}$ is said to be *alternating* if $\mathcal{L}$ admits an alternating diagram.

Traditionally, one indexes tables of prime (meaning non-composite, see Figure 1) knots by the crossing number, with a subscript to indicate which particular knot out of those with this many crossings one means. In the tables, one counts mirror images as a single knot type. We use the Rolfsen table (see [8]) for knots with ≤ 10 crossings and the KnotScape table (see [10]) for knots with ≥ 11 crossings.

The majority of knots with ≤ 9 crossings are alternating. In particular, there are only 3 non-alternating knots 8_{19}, 8_{20}, and 8_{21} among the 36 prime knots with ≤ 8 crossings, and there are only 8 non-alternating knots $9_{42}, 9_{43}, \dots, 9_{49}$ among the 49 prime knots with 9 crossings. Nevertheless, as the crossing number increases, the percentage of prime knots that are alternating goes to 0 exponentially quickly (see Theorem 1 in [48]).

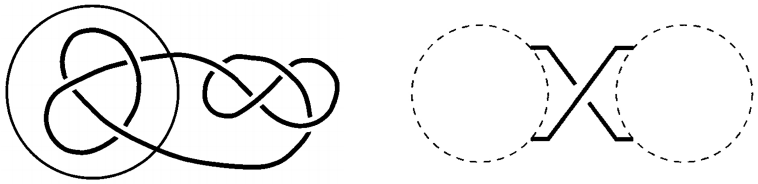

FIGURE 1. A composite link diagram (on the left). An isthmus (on the right).

A diagram $\mathcal{D}$ is said to be *reduced* if $\mathcal{D}$ has no isthmuses (see Figure 1). If $\mathcal{D}$ is not reduced, one can apply an obvious transformation that reduces the number of crossings. Therefore, any minimal diagram is reduced.

The original compilations of knot tables by P. G. Tait and C. N. Little at the end of the 19th century gave reason to believe that any reduced alternating diagram is minimal. This well-known fact, referred to as the *first Tait conjecture*, was proved in 1987 by L. Kauffman, M. B. Thistlethwaite, and K. Murasugi independently by using the *Jones polynomial* for links (see Theorem 2.10 in [35], Theorem 2 in [36], and Theorem A in [37]). Namely, they showed that the number of crossings of any diagram of a link $\mathcal{L}$ is bounded from below by the difference between the highest and the lowest degrees of the Jones polynomial $\mathcal{V}_L(t)$ of $\mathcal{L}$. Moreover, for any reduced alternating link diagram, the equality holds.

In [38] (see Corollary 3.4), M. B. Thistlethwaite used a generalization of the Jones polynomial, referred to as the *Kauffman polynomial*, and obtained similar minimality results for a more general class of links, which are called *adequate*. Note that the precise definition is

visual, that is, given a link diagram $\mathcal{D}$, it is easy to verify whether $\mathcal{D}$ is adequate. All reduced alternating diagrams are adequate. The simplest adequate non-alternating prime knots have 10 crossings, and there are 3 such: 10_{152}, 10_{153}, and 10_{154}.

It is noteworthy that if a prime diagram is not alternating, the inequality above is strict. The latter implies that any minimal diagram of each prime alternating link is alternating. By using this, in [39] (see Theorem 10), the authors showed that some specific link diagrams, referred to as *reduced*[1] *Montesinos* ones, are minimal.

Another class of minimal diagrams is of some closed braids. We denote by $\mathcal{B}_n$ the braid group with n strands. Recall that $\mathcal{B}_n$ admits the following presentation with standard Artin generators:

$$\mathcal{B}_n = \langle \sigma_1, \dots, \sigma_{n-1} \mid \sigma_i\sigma_{i+1}\sigma_i = \sigma_{i+1}\sigma_i\sigma_{i+1},\ 1 \le i \le n-1;\ \sigma_i\sigma_j = \sigma_j\sigma_i,\ |i-j| \ge 2 \rangle.$$

The relation $\sigma_k\sigma_{k+1}\sigma_k = \sigma_{k+1}\sigma_k\sigma_{k+1}$ is called the *braid relation*, and the relation $\sigma_i\sigma_j = \sigma_j\sigma_i$ is called the *far commutativity* relation. An element of $\mathcal{B}_n$ is called a *braid* with n strands. Given a set of symbols S, denote by S^* the set of all words in the alphabet S. An element of $\{\sigma_1, \dots, \sigma_{n-1}, \sigma_1^{-1}, \dots, \sigma_{n-1}^{-1}\}^*$ is called a *braid word in* $\mathcal{B}_n$.

We visualize braid words by their diagrams, which one draws vertically from top to bottom. For example, see the second picture in Figure 2 for the braid diagram corresponding to $\sigma_2\sigma_3\sigma_2\sigma_1^{-1}\sigma_3\sigma_2\sigma_3\sigma_2\sigma_1^{-1}$. It is easy to see that there is a correspondence between the far commutativity classes of braid words and the plane isotopy classes of braid diagrams. By abusing the notation, one treats braid diagrams as braid words.

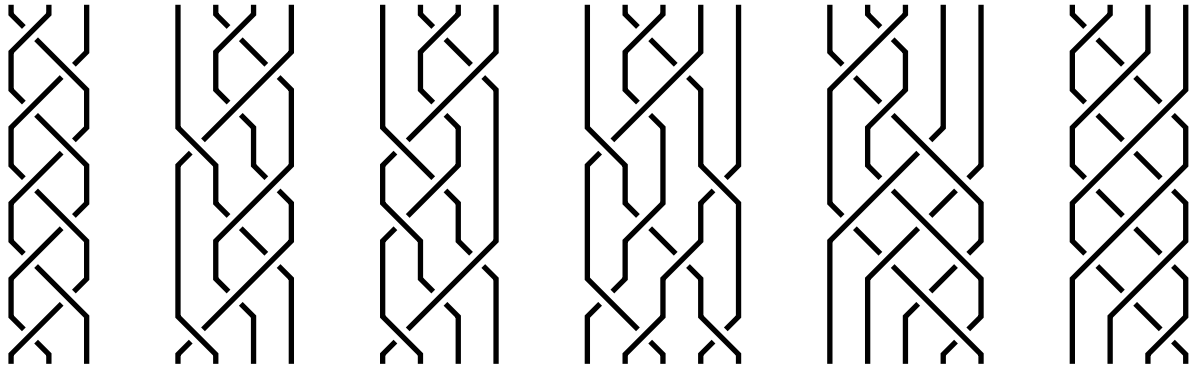

FIGURE 2. Examples of braid diagrams.

In [31], J. Gonzàlez-Meneses and P. M. G. Manchòn introduced a new class of braid diagrams, which we call the *GMM* ones. By definition, a braid word $w \in \{\sigma_1, \dots, \sigma_{n-1}\}^*$ corresponds to a GMM braid diagram if any only if one can obtain w from the empty word by a finite sequence of transformations of the following types:

(1) for some $i \in \{1, 2, \dots, n-1\}$, inserting $\sigma_i\sigma_i$;
(2) for some $i \in \{1, 2, \dots, n-1\}$, doubling a letter σ_i;
(3) applying either the braid relation or the far commutativity one.

See the rightmost picture in Figure 2 for an example of a GMM braid diagram.

Any braid diagram gives rise to a link diagram via the *Alexander closure*, see Figure 3. We endow the resulting link diagram with a natural downward orientation.

[1] In [39], *reduced* means something different to that of the present thesis.

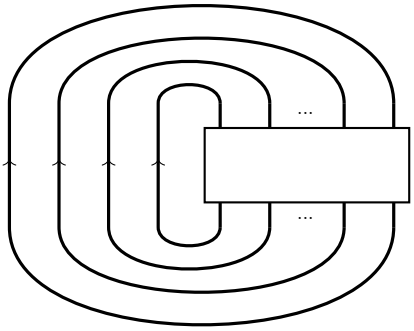

FIGURE 3. The Alexander closure of a braid diagram.

A link diagram $\mathcal{D}$ is called a *GMM diagram* if $\mathcal{D}$ is the Alexander closure of a GMM braid diagram. For example, up to mirror images, any torus link admits a GMM diagram. All GMM diagrams are minimal. In their research, J. Gonzàlez-Meneses and P. M. G. Manchòn used the *skein polynomial*, which is a generalization of the Jones polynomial. We discuss this approach in the next subsection.

Another class of diagrams is that of homogeneous ones, which was introduced in [11].

We assume that all link diagrams are oriented and lie on an oriented 2-sphere S^2. A crossing is said to be positive (resp. negative) if it has the form on the left (resp. right) picture in Figure 4.

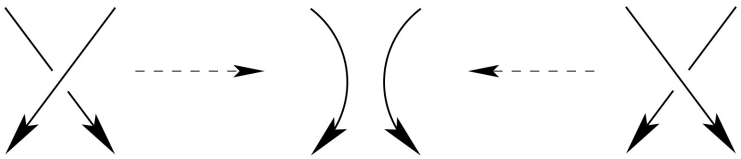

FIGURE 4. Smoothing of a crossing.

Let $\mathcal{D}$ be a link diagram. After smoothing all crossings of $\mathcal{D}$, one obtains finitely many simple closed curves, which are called *Seifert circles* of $\mathcal{D}$.

Let $\Gamma(\mathcal{D})$ be a graph whose vertex set is the set of all Seifert circles of $\mathcal{D}$ and whose edges correspond to crossings of $\mathcal{D}$.

Recall that a vertex of a finite graph is said to be a *cut vertex* if, as one removes it, the number of connected components of the graph increases. Let G be a finite graph. A subgraph H of G is called a *block* of G if, first, H is connected; second, H has no cut vertices; third, H is maximal for these properties.

A block H of $\Gamma(\mathcal{D})$ is said to be *homogeneous* if all edges of H have the same crossing type, which is either positive or negative. The diagram $\mathcal{D}$ is said to be *homogeneous* if each block of $\Gamma(\mathcal{D})$ is homogeneous.

For example, any alternating diagram is homogeneous.

A diagram $\mathcal{D}$ is said to be *positive* if all crossings of $\mathcal{D}$ are positive. A link $\mathcal{L}$ is said to be *homogeneous* (resp. positive) if $\mathcal{L}$ admits a homogeneous (resp. positive) diagram.

Note that all prime knots up to nine crossings except 8_{20}, 8_{21}, 9_{42}, 9_{44}, 9_{45}, 9_{46}, and 9_{48} are homogeneous.

Homogeneous links admit the following equivalent definition. The Seifert circles of a link diagram $\mathcal{D}$ divide the 2-sphere into regions. We say that $\mathcal{D}$ is *uniform* if, within each such region, all crossings of $\mathcal{D}$ have the same type. If $\mathcal{D}$ is uniform, then $\mathcal{D}$ is homogeneous. In general, the converse does not hold. However, for any homogeneous diagram $\mathcal{D}$, one can use flips to transform $\mathcal{D}$ into a new diagram $\mathcal{D}'$ representing the same link such that $\mathcal{D}'$ is uniform. Thus, a link $\mathcal{L}$ is homogeneous if and only if $\mathcal{L}$ admits a uniform diagram.

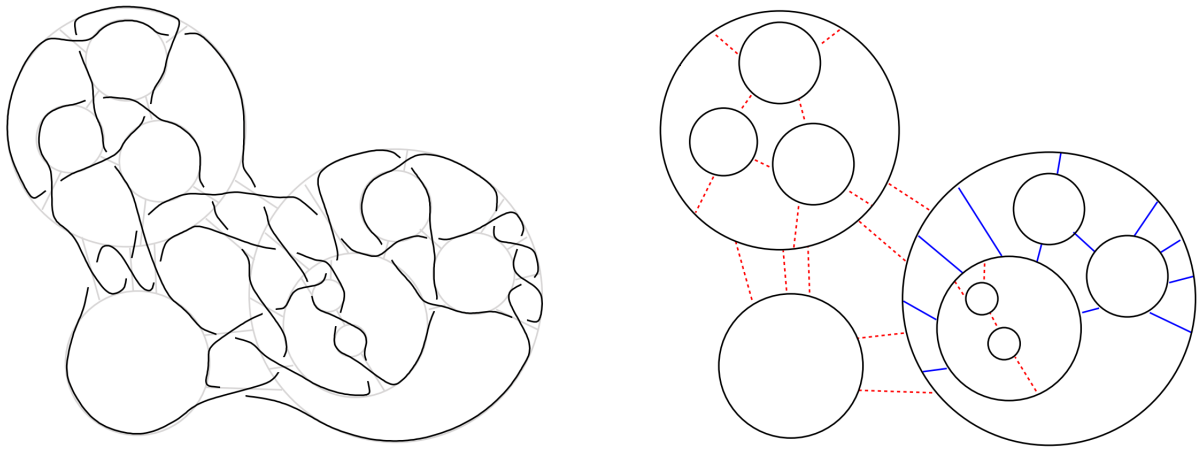

FIGURE 5. An example of a homogeneous link diagram $\mathcal{D}$ (on the left). The union of Seifert circles of $\mathcal{D}$ with an indication of crossing types (on the right). The orientation is omitted. The picture was taken from [18].

In contrast to alternating diagrams, there are non-minimal reduced homogeneous ones (for example, see Figure 12 in [11]). Also, some positive links admit both non-minimal positive diagrams and non-homogeneous minimal ones (for example, $11n_{183}$, see [26]). In [11] (see Questions 1 and 2), the author suggests studying minimal diagrams of homogeneous links. Our results show that there are sufficient conditions on a homogeneous diagram so that it is minimal. In particular, we describe a new class of minimal homogeneous diagrams.

Let us provide more reasons to study homogeneous diagrams. A natural question is whether one can read off topological properties of the link given by a diagram $\mathcal{D}$ (such as knottedness, splitness, and primeness) from $\mathcal{D}$.

In some sense, homogeneous links are visually knotted. Namely, a homogeneous link $\mathcal{L}$ is trivial if and only if for some (and hence any) homogeneous diagram $\mathcal{D}$ of $\mathcal{L}$, $\Gamma(\mathcal{D})$ has no cycles (see Theorem 3 in [11] and Corollary 7.6.3 in [3]). Recall that a link $\mathcal{L}$ is said to be *split* if $\mathcal{L}$ admits a disconnected diagram. Homogeneous links are visually split, that is, a homogeneous link $\mathcal{L}$ is split if and only if some (and hence any) homogeneous diagram of $\mathcal{L}$ is disconnected (see Corollary 3.1 in [11] and Corollary 7.6.4 in [3]). Finally, in [15], the author conjectured that homogeneous links are visually prime, that is, a homogeneous link $\mathcal{L}$ is prime if and only if some (and hence any) homogeneous diagram of $\mathcal{L}$ is prime. The conjecture holds for both alternating (see Theorem 1 in [16] and Theorem 4.4 in [6]) and positive links (see Theorem 1.4 in [14] and Theorem 1.2 in [15]).

In contrast to alternating links, for homogeneous ones, many questions remain unsolved. In particular, no analog of the flyping conjecture (see below) has been found for homogeneous links so far.

1.1. **The skein polynomial.** Before introducing the main results of the present thesis, we need some more preliminaries.

In [24, 25], the authors proved that there is a unique function that maps each link diagram $\mathcal{D}$ to a two-variable Laurent polynomial $P(\mathcal{D};a,z)\in\mathbb{Z}[a^{\pm1},z^{\pm1}]$ such that:

(1) If two link diagrams $\mathcal{D}$ and $\mathcal{D}'$ represent the same link, then $P(\mathcal{D};a,z)=P(\mathcal{D}';a,z)$.
(2) One has
$$aP(\mathcal{D}_+;a,z)-a^{-1}P(\mathcal{D}_-;a,z)=zP(\mathcal{D}_0,a,z)$$
whenever $\mathcal{D}_+$, $\mathcal{D}_0$, and $\mathcal{D}_-$ are link diagrams that coincide except at a small region where the diagrams are presented as in Figure 4, respectively.
(3) If $\mathcal{D}$ is a knot diagram without crossings, then $P(\mathcal{D};a,z)=1$.

The polynomial $P(\mathcal{D};a,z)$ is referred to as the *skein polynomial*, the *HOMFLY polynomial*, the *HOMFLY-PT polynomial*, the *generalized Jones polynomial*, and the *twisted Alexander polynomial* of $\mathcal{D}$. The second condition is referred to as the *skein relation*.

Given a link $\mathcal{L}$, let $P(\mathcal{L};a,z):=P(\mathcal{D};a,z)$ for some (and hence any) diagram $\mathcal{D}$ of $\mathcal{L}$. The skein polynomial is a generalization of the Jones polynomial. Namely, for any link $\mathcal{L}$, one has
$$V_{\mathcal{L}}(t)=P(\mathcal{L};t,t^{1/2}-t^{-1/2}).$$

Denote by $s(\mathcal{D})$ the number of Seifert circles of $\mathcal{D}$ and by $|\mathcal{D}|$ the number of crossings of $\mathcal{D}$. Denote by $\omega(\mathcal{D})$ the *writhe* of $\mathcal{D}$, that is, the difference between the number of positive and the number of negative crossings of $\mathcal{D}$. A diagram $\mathcal{D}$ of a link $\mathcal{L}$ is said to be *optimal* if $\mathcal{D}$ has the least number of Seifert circles among all diagrams of $\mathcal{L}$.

The relationship between $s(\mathcal{D})$ and the skein polynomial is analogous to the relationship between $|\mathcal{D}|$ and the Jones polynomial. The analogy is as follows.

Let $Q_i(\mathcal{L};z)\in\mathbb{Z}[z^{\pm1}]$ be polynomials such that $P(\mathcal{L};a,z)=\sum_{i=e}^{E}Q_i(\mathcal{L};z)a^i$, $Q_e(\mathcal{L};z)\neq0$, and $Q_E(\mathcal{L};z)\neq0$. In [29] (see Theorem 1), the author proved that for any diagram $\mathcal{D}$ of $\mathcal{L}$, one has
$$-\omega(\mathcal{D})-(s(\mathcal{D})-1)\le e\le E\le-\omega(\mathcal{D})+(s(\mathcal{D})-1). \tag{1.1}$$
In particular,
$$(E-e)/2+1\le s(\mathcal{D}). \tag{1.2}$$
The latter is referred to as the *Morton–Franks–Williams inequality*. Given a link diagram $\mathcal{D}$, we say that (1.2) is *sharp* for $\mathcal{D}$ if $(E-e)/2+1=s(\mathcal{D})$. In this case, $\mathcal{D}$ is optimal. Note that (1.2) is sharp if and only if both outer inequalities in (1.1) are sharp.

Note that all prime knots up to 10 crossings except 9_{42}, 9_{49}, 10_{132}, 10_{150}, and 10_{156} admit diagrams, for which the Morton–Franks–Williams inequality (1.2) is sharp. The same is true for all closed positive braids with ≤3 strands (see Proposition 3.1 in [33]), fibered alternating links (see Theorem A in [28]), rational links (see Theorem B in [28]), and GMM ones (see Corollary 4.3 in [31]). Also, in [31], the authors proved that given a positive braid diagram $\mathcal{D}$, the Morton–Franks–Williams inequality (1.2) is sharp for the Alexander closure of $\mathcal{D}$ if and only if $\mathcal{D}$ is a GMM braid diagram.

Let $P_i(\mathcal{L};a)\in\mathbb{Z}[a^{\pm1}]$ be polynomials such that $P(\mathcal{L};a,z)=\sum_{i=m}^{M}P_i(\mathcal{L};a)z^i$, $P_m(\mathcal{L};a)\neq0$, and $P_M(\mathcal{L};a)\neq0$. In [29] (see Theorem 2), the author proved that for any diagram $\mathcal{D}$ of $\mathcal{L}$, one has
$$M\le|\mathcal{D}|-s(\mathcal{D})+1. \tag{1.3}$$

By combining (1.2) and (1.3), one has

$$M + (E - e)/2 \le |\mathcal{D}|.$$

Remark 1.1. The inequality (1.3) is sharp for all homogeneous diagrams (see Theorem 4 in [11], Theorem 7.6.2 in [3], and Theorem 6 in [12]). Besides, (1.3) is sharp for an almost positive diagram of a prime knot $12n_{149}$, which is not homogeneous.

Remark 1.2. Suppose (1.3) is sharp for $\mathcal{D}$. If $\mathcal{D}$ is optimal, then $\mathcal{D}$ is minimal. Indeed, for any diagram $\mathcal{D}'$ of the same link $\mathcal{L}$, one has

$$|\mathcal{D}| = M + s(\mathcal{D}) - 1 \le (|\mathcal{D}'| - s(\mathcal{D}') + 1) + s(\mathcal{D}) - 1 \le |\mathcal{D}'|.$$

This result was firstly observed in [28] (see Proposition 7.4). Moreover, in this case, any minimal diagram of $\mathcal{L}$ is optimal. Indeed, for any minimal diagram $\mathcal{D}'$ of $\mathcal{L}$, one has

$$s(\mathcal{D}') \le |\mathcal{D}'| - M + 1 = |\mathcal{D}'| - (|\mathcal{D}| - s(\mathcal{D}) + 1) + 1 = s(\mathcal{D}).$$

1.2. **Braids and links.** We follow [49] and generalize the Alexander closure of braids construction. By using this construction, in the next subsection, we describe a new class of link diagrams, for which the Morton–Franks–Williams inequality (1.2) is sharp.

Let $\mathcal{C} = \{C_1, C_2, \dots, C_s\}$ be a set of disjoint oriented circles on the 2-sphere S^2 and

$$\|\cdot\| : \mathcal{C} \longrightarrow \{1, 2, \dots\}$$

be an arbitrary function, which is referred to as a *weight function*. Let $\mathcal{A} = \{\alpha_1, \alpha_2, \dots, \alpha_t\}$ be a set of disjoint oriented simple closed arcs on S^2. A triple $(\mathcal{C}, \mathcal{A}, \|\cdot\|)$ is called a *system of weighted circles* if for all $i \in \{1, 2, \dots, s\}$, $j \in \{1, 2, \dots, t\}$, and $x \in (C_i \cap \alpha_j) \cup \partial\alpha_j$, there is a neighborhood of x diffeomorphic to one of the pictures shown in Figure 6.

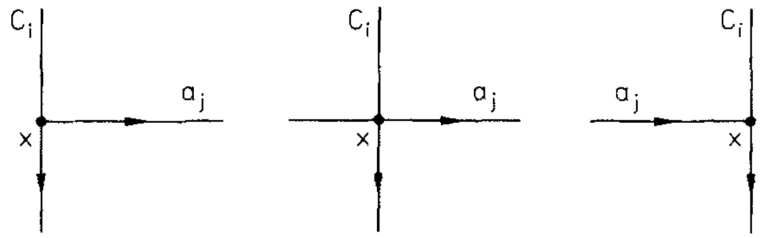

FIGURE 6. Any point $x \in (C_i \cap \alpha_j) \cup \partial\alpha_j$ has a neighborhood that looks like one of these.

Let $(\mathcal{C}, \mathcal{A}, \|\cdot\|)$ be a system of weighted circles. Given $\alpha \in \mathcal{A}$, denote by $\|\alpha\|$ the sum of weights of all circles intersecting α. Note that for all $\alpha \in \mathcal{A}$, the arc α intersects each circle $C \in \mathcal{C}$ no more than once, and $\|\alpha\| \ge 2$. A function

$$\pi : \mathcal{A} \longrightarrow \{\sigma_i^{\pm 1} \mid i \in \{1, 2, 3, \dots\}\}^*$$

is called a *braid placement* if for all $\alpha \in \mathcal{A}$, one has

$$\pi(\alpha) \in \{\sigma_i^{\pm 1} \mid i \in \{1, 2, \dots, \|\alpha\| - 1\}\}^*.$$

Any braid placement π determines a link diagram as follows. First, for each $C \in \mathcal{C}$, replace C by $\|C\|$ concentric circles (see Figure 7). Second, for each $\alpha \in \mathcal{A}$, insert a braid diagram corresponding to $\pi(\alpha)$ according to the orientation. We say that the resulting link is determined by π. Note that any link diagram arises this way.

Let $(\mathcal{C}, \mathcal{A}, \|\cdot\|)$ be a system of weighted circles. Each connected component of

$$\left(\bigcup_{C\in\mathcal{C}} C\right) \cup \left(\bigcup_{\alpha\in\mathcal{A}} \alpha\right)$$

determines a division of S^2 into regions. The system $(\mathcal{C}, \mathcal{A}, \|\cdot\|)$ is said to be *reduced* if, for each such connected component, no topological disk region has precisely four distinct sides.

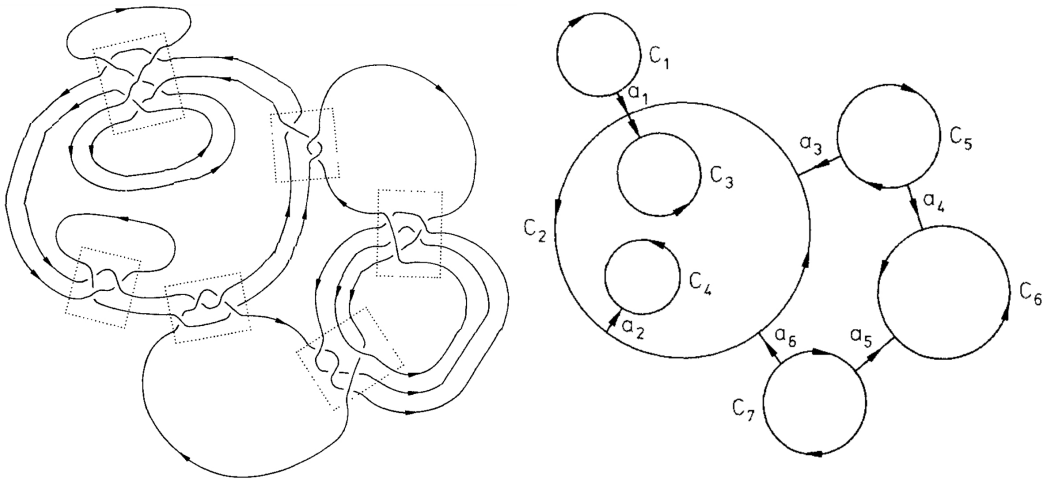

FIGURE 7. A link diagram determined by a braid placement.

1.3. **Solid links.** In this subsection, we describe our main results concerning the new class of link diagrams, referred to as *solid* ones.

In [50], J. Stallings introduced the concept of homogeneous braid words. Namely, given $r_1, \dots, r_{n-1} \in \{1, -1\}$, a braid word w is said to be $(r_1, \dots, r_{n-1})$-homogeneous if w contains none of the letters $\sigma_1^{-r_1}, \sigma_2^{-r_2}, \dots, \sigma_{n-1}^{-r_{n-1}}$. We say that a word w is *homogeneous* whenever w is $(r_1, \dots, r_{n-1})$-homogeneous for some $r_1, \dots, r_{n-1}$. A braid is said to be *homogeneous* if it has a homogeneous braid word representative.

For example, any positive braid diagram is homogeneous. It is easy to check that the Alexander closure of a homogeneous braid diagram is a homogeneous link diagram.

Given $i, j \in \{1, 2, \dots, n\}$ such that $i < j$, let

$$\delta_{i,j} := (\sigma_i\sigma_{i+1}\dots\sigma_{j-1}\sigma_j)(\sigma_i\sigma_{i+1}\dots\sigma_{j-1})\dots(\sigma_i\sigma_{i+1})\sigma_i. \tag{1.4}$$

The braid $\Delta_{1,n}$ determined by $\delta_{1,n}$ is referred to as the *half twist*, the *fundamental braid*, and the *Garside element* in B_n. The braid $\Delta_{1,n}^2$ is referred to as the *full twist*.

Let $r_1, \dots, r_{n-1} \in \{1, -1\}$. Let $i_1, i_2, \dots, i_m \in \{1, 2, \dots, n\}$ be such that $1 = i_1 < i_2 < \dots < i_m = n$ and for all $k \in \{1, 2, \dots, m-1\}$, one has $r_{i_k} = r_{i_k+1} = \dots = r_{i_{k+1}-1}$ and $r_{i_{k+1}-1} \neq r_{i_{k+1}}$.

Let $\mathcal{H}^+(r_1, \dots, r_{n-1})$ (resp. $\mathcal{H}^-(r_1, \dots, r_{n-1})$) be the class of all $(r_1, \dots, r_{n-1})$-homogeneous braid words w such that for each $k \in \{1, 2, \dots, m-1\}$ such that $r_{i_k} = 1$ (resp. $r_{i_k} = -1$), the braid word obtained from w by deleting all letters except $\sigma_{i_k}^{\pm 1}, \sigma_{i_k+1}^{\pm 1}, \dots, \sigma_{i_{k+1}-1}^{\pm 1}$ admits a decomposition of the form $v_1v_2v_3$ such that both v_1 and v_3 represent $\Delta_{i_k,i_{k+1}}$ (resp. $\Delta_{i_k,i_{k+1}}^{-1}$).

Let $\mathcal{H}^+$ (resp. $\mathcal{H}^-$) be the union of all $\mathcal{H}^+(r_1, \dots, r_{n-1})$ (resp. $\mathcal{H}^-(r_1, \dots, r_{n-1})$), where $n \geq 2$ and $r_1, \dots, r_{n-1} \in \{1, -1\}$. An element of $\mathcal{H}^+$ (resp. $\mathcal{H}^-$) is called a $+$*solid* (resp. $-$*solid*) braid word. An element of $\mathcal{H}^+ \cap \mathcal{H}^-$ is called a *solid* braid word.

For example, all braid diagrams shown in Figure 2 correspond to solid braid words.

Definition 1.3. Let $\# \in \{+,-\}$. Let $(\mathcal{C},\mathcal{A},\|\cdot\|)$ be a reduced system of weighted circles and π be a braid placement. The braid placement π is said to be *#solid* (resp. *solid*) if for all $\alpha \in \mathcal{A}$, one has $\pi(\alpha) \in \mathcal{H}^{\#}$ (resp. $\pi(\alpha) \in \mathcal{H}^{+} \cap \mathcal{H}^{-}$). In this case, the link diagram $\mathcal{D}$ determined by π is said to be *#solid* (resp. *solid*). A link is said to be *solid* if it admits a solid diagram.

By using methods of [1, 2], we show that all solid diagrams are optimal. In particular, those of them, for which (1.3) is sharp, are minimal. For the corresponding links, the crossing number is equal to $M + (E - e)/2$.

Theorem 1.4. The Morton–Franks–Williams inequality (1.2) is sharp for all solid diagrams.

Corollary 1.5. All solid diagrams are optimal.

Remarks 1.1 and 1.2 imply the following results.

Corollary 1.6. All solid homogeneous diagrams are minimal.

Corollary 1.7. The Alexander closure of a homogeneous braid diagram is minimal whenever the corresponding braid word is solid.

For example, all closed positive braid diagrams with the full twist are solid. The sharpness result for them is well known (see Corollary 2.4 in [30], Theorem 10.5.1 in [3], Corollary 4.5 in [31], Theorem 1.3 in [32], and Corollary 1.4 in [34]). In particular, all torus links are solid.

If for a link diagram $\mathcal{D}$, there exist two Seifert circles that share exactly one common crossing, then $\mathcal{D}$ is not optimal. Namely, one can apply a transformation that reduces the number of Seifert circles. The transformation is referred to as the *Murasugi–Przytycki move* (see Definition 2.1 in [27]).

It follows that some reduced alternating (and hence minimal) diagrams are not optimal (compare with Remark 1.2 above). Still, if for an alternating diagram $\mathcal{D}$, any two Seifert circles of $\mathcal{D}$ have either no common crossings or at least two common crossings, then the corresponding alternating link is solid. The sharpness of the Morton–Franks–Williams inequality (1.2) for solid alternating links was firstly observed in [2] (see Theorem 1.1).

The non-homogeneous solid diagram $\mathcal{D}$ shown in Figure 8 is minimal, but (1.3) is not sharp for $\mathcal{D}$. At the same time, there exist non-minimal solid diagrams.

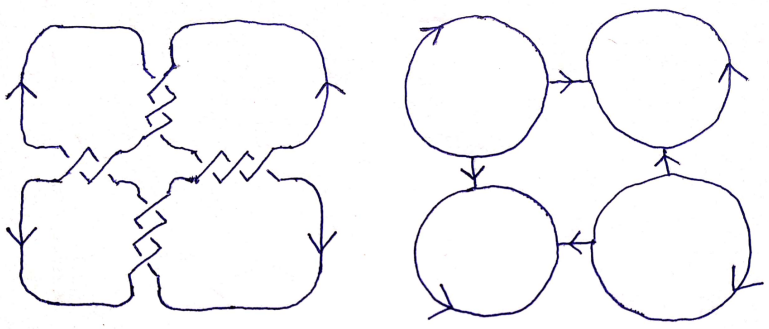

FIGURE 8. A solid non-homogeneous diagram of $11n_{74}$ and the corresponding system of weighted circles.

Among the 36 prime knots with ≤ 8 crossings, there are 4 torus and 14 solid alternating ones. Besides, among the 49 prime knots with 9 crossings, there are 1 torus and 16 solid alternating ones. The second and the third braid diagrams shown in Figure 2 provide solid homogeneous

diagrams of 9_{43} and 9_{47}. Both 9_{43} and 9_{47} admit neither adequate nor reduced Montesinos nor GMM link diagrams. Thus, Corollary 1.7 provides the first non-brute-force proof of the following result.

Corollary 1.8. The crossing number of both 9_{43} and 9_{47} is 9.

A well-known conjecture states that the crossing number is additive under connected sums, that is, connected sums of minimal link diagrams are minimal (see Problem 1.65 in [19], [20], and p. 69 in [9]). The latter is still open in general. Since connected sums of adequate (resp. GMM) diagrams are adequate (resp. GMM), the conjecture holds for both adequate and GMM diagrams. Also, connected sums of minimal diagrams of torus links are minimal (see Theorem 3.8 in [21] and Corollary 3.6 in [22]). Note that connected sums of solid homogeneous diagrams are solid homogeneous. Corollary 1.6 implies the following result.

Corollary 1.9. The conjecture that the crossing number is additive under connected sums holds for all solid homogeneous links.

Following [23], we say that a minimal diagram $\mathcal{D}$ is 1-*regular* if for any diagram $\mathcal{D}'$, the crossing numbers of links determined by connected sums of $\mathcal{D}$ and $\mathcal{D}'$ are bounded from below by the number of crossings of $\mathcal{D}$. If the additivity of crossing number conjecture holds, then any minimal link diagram is 1-regular. By using properties of the Kauffman polynomial, one can show that all adequate diagrams are 1-regular. Also, all minimal diagrams of torus links are 1-regular (see Theorem 3.8 in [21]). In [21] (see Theorem 3.8), the author provided a sufficient condition on a link diagram to be 1-regular. By using Corollary 4.1 in [11], one can show that optimal homogeneous diagrams satisfy the condition. In particular, all GMM diagrams are 1-regular. Also, Corollary 1.5 implies the following result.

Corollary 1.10. All solid homogeneous diagrams are 1-regular.

Our next step is to study minimal diagrams of solid links. Recall that any minimal diagram of a prime alternating link is alternating and that some positive links admit non-positive minimal diagrams. Still, any minimal diagram of an alternating link is homogeneous. We propose the following conjecture.

Conjecture 1.11. Suppose a link $\mathcal{L}$ admits a solid homogeneous diagram. Then any minimal diagram of $\mathcal{L}$ is homogeneous.

It is not hard to check that if the Morton–Franks–Williams inequality (1.2) is sharp for a link diagram $\mathcal{D}$, then any two optimal diagrams of $\mathcal{L}$ have the same writhe. In particular (see Remark 1.2), any minimal diagram of a solid positive link is positive. Thus, Conjecture 1.11 holds for all solid positive links.

1.4. **Homogeneous braids.** In this subsection, we describe our results concerning braid diagrams. The latter provide reasons to believe that Conjecture 1.11 holds.

Let us introduce the following equivalence relations on the set of all braid diagrams with n strands:

(1) to represent the same element of $\mathcal{B}_n$;
(2) to represent conjugate elements of $\mathcal{B}_n$;
(3) to represent the same link via the Alexander closure.

Note that (1) implies (2) and (2) implies (3). One treats equivalence classes generated by the second equivalence relation as braids in the solid torus $[0,1]\times[0,1]\times S^1$.

A braid diagram is said to be *minimal* if it has the least possible number of crossings among all braid diagrams representing the same braid. The number of crossings of a minimal diagram of a braid is called the crossing number of the braid. A braid $\beta \in \mathcal{B}_n$ is said to be of *minimal conjugacy length* if β has the smallest crossing number among all braids in the conjugacy class $\{\delta^{-1}\beta\delta \mid \delta \in \mathcal{B}_n\}$. A braid diagram $\mathcal{D}$ is said to be of *minimal conjugacy length* if $\mathcal{D}$ is minimal, and the corresponding braid is of minimal conjugacy length.

Proposition 1.12. Let $r_1, \dots, r_{n-1} \in \{1, -1\}$ and β be a $(r_1, \dots, r_{n-1})$-homogeneous braid. A diagram $\mathcal{D}$ of β is minimal if and only if $\mathcal{D}$ is $(r_1, \dots, r_{n-1})$-homogeneous.

Corollary 1.13. A diagram $\mathcal{D}$ of a homogeneous braid is minimal if and only if $\mathcal{D}$ is homogeneous.

A basis of the proof of Proposition 1.12 is an analog of the Conway polynomial for tangles.

Proposition 1.14. Let β be a homogeneous braid. A diagram $\mathcal{D}$ of a braid in $\{\delta^{-1}\beta\delta \mid \delta \in B_n\}$ is of minimal conjugacy length if and only if $\mathcal{D}$ is homogeneous.

A basis of the proof of Proposition 1.12 is a three-variable polynomial invariant of braids, constructed in [41].

Note that some closed solid homogeneous braids admit non-braid-like minimal diagrams. For example, both 10_{138} and $12n_{706}$ admit both closed solid homogeneous braid diagrams (see the fourth and the fifth diagrams in Figure 2) and minimal diagrams whose Seifert circles are not concentric. However, all minimal knot diagrams of both 10_{138} and $12n_{706}$ are homogeneous.

2. The skein polynomial of solid links

In this section, we prove Theorem 1.4.

Recall a general principle that is used to calculate the skein polynomial. For a trivial link diagram $\mathcal{D}$ with n components, it is not hard to show that $\mathcal{P}(\mathcal{D}; a, z) = ((a - a^{-1})z^{-1})^{n-1}$.

Given a link diagram $\mathcal{D}$, let $\mathcal{T}$ be a rooted and edge-weighted binary tree, which is directed from a root, such that:

(1) each vertex of $\mathcal{T}$ is a link diagram;
(2) the root vertex of $\mathcal{T}$ is $\mathcal{D}$;
(3) each leaf vertex of $\mathcal{T}$ represents an unlink;
(4) each internal vertex has exactly two children vertices. The corresponding three link diagrams are identical except at one crossing, and they are related by one of the two possible relations at that crossing, as shown in Figure 9.

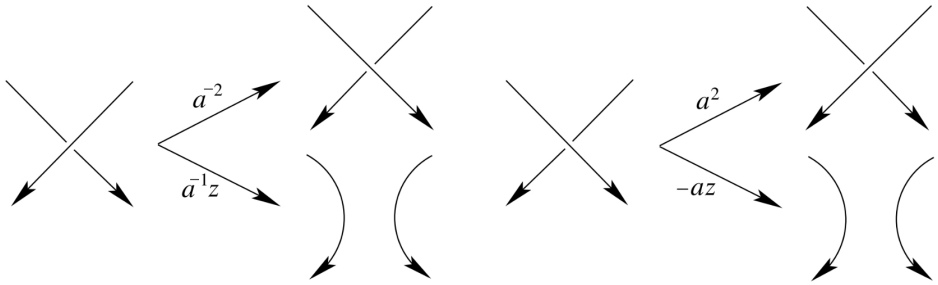

Figure 9. The edge weight assignment for a resolving tree.

The tree $\mathcal{T}$ is called a *resolving tree* (for the skein polynomial) of $\mathcal{D}$. One treats the resolving tree as a parsing tree.

Any link diagram admits a resolving tree (see below). In general, there are several resolving trees for a given diagram.

Remark 2.1. Any resolving tree $\mathcal{T}$ of $\mathcal{D}$ gives rise to a decomposition of $\mathcal{P}(\mathcal{D};a,z)$ as a sum, which is indexed by leaf vertices of $\mathcal{T}$, as follows. Note that the skein relation admits the following equivalent forms:

$$\mathcal{P}(\mathcal{D}_+;a,z) = a^{-2}\mathcal{P}(\mathcal{D}_-;a,z) + a^{-1}z\mathcal{P}(\mathcal{D}_0,a,z),$$
$$\mathcal{P}(\mathcal{D}_-;a,z) = a^{2}\mathcal{P}(\mathcal{D}_+;a,z) - az\mathcal{P}(\mathcal{D}_0,a,z).$$

Let $\mathcal{U}$ be a leaf vertex of $\mathcal{T}$. Denote by $\gamma(\mathcal{U})$ the number of link components of $\mathcal{U}$. Let P be a unique path on $\mathcal{T}$ from the root vertex $\mathcal{D}$ to the leaf vertex $\mathcal{U}$. It is easy to see that the contribution of $\mathcal{U}$ to $\mathcal{P}(\mathcal{D};a,z)$ is $((a-a^{-1})z^{-1})^{\gamma(\mathcal{U})-1}$ multiplied by the weights of the edges in P. Let $t(\mathcal{U})$ be the number of crossings of $\mathcal{D}$ that one smoothed in obtaining $\mathcal{U}$, and $t^-(\mathcal{U})$ be the number of negative crossings among the smoothed ones. As Figure 9 shows, the degree of a in the weight of an edge is exactly the change of writhe from the starting vertex of the edge to the ending vertex of the edge. Also, a z term in the weight of the edge indicates that the ending vertex is obtained from the starting vertex by a crossing smoothing and a negative sign in the weight indicates that the smoothed crossing is negative. It follows that

$$\mathcal{P}(\mathcal{D};a,z) = \sum_{\mathcal{U}\in\mathcal{T}_\circ} (-1)^{t^-(\mathcal{U})} z^{t(\mathcal{U})} a^{\omega(\mathcal{U})-\omega(\mathcal{D})} ((a-a^{-1})z^{-1})^{\gamma(\mathcal{U})-1},$$

where $\mathcal{T}_\circ$ is the set of leaf vertices of $\mathcal{T}$.

Remark 2.2. We think of a resolving tree as a graph of a branching process (in the sense of probability theory). Namely, at each internal vertex, one takes a crossing of the current link diagram and branch on smoothing and flipping the crossing. Hence, to construct a resolving tree, one can describe a rule that determines the corresponding crossings of intermediate link diagrams. The rule determines the evolution of the branching process.

With this idea in mind, we describe resolving trees introduced in [2].

2.1. **Two special classes of resolving trees.** By a point on a link diagram $\mathcal{D}$, we mean a point x on an arc of $\mathcal{D}$ such that x is not a crossing. By a point on a Seifert circle C of $\mathcal{D}$, we mean a point x on the intersection of C and $\mathcal{D}$.

Let $\mathcal{U}$ be a link diagram and $m = \gamma(\mathcal{D})$. Let $p_1, p_2, \ldots, p_m$ be a sequence of base points on $\mathcal{U}$ such that for $i \neq j$, the points p_i and p_j lie on distinct components of $\mathcal{U}$. One may travel through $\mathcal{D}$ by moving through each such component as follows. One starts at the first marked point p_1 and moves according to the orientation. As one reaches p_1 again, one chooses the second marked point p_2, starts moving according to the orientation. Then one continues similarly. Such travel is said to be *natural*.

During this process, one visits each crossing of $\mathcal{U}$ exactly twice. A crossing of $\mathcal{U}$ is said to be *descending* (resp. *ascending*), if one travels along the overpassing (resp. underpassing) strand first. The diagram $\mathcal{U}$ is said to be *descending* (resp. *ascending*) if each crossing of $\mathcal{U}$ is descending (resp. ascending). Note that if $\mathcal{U}$ is descending (resp. ascending), then the components of $\mathcal{U}$ are both layered from top to bottom (resp. from bottom to top) and represent unknots. In this case, $\mathcal{U}$ represents an unlink.

Choose an arbitrary base point x on $\mathcal{U}$. Then travel through $\mathcal{U}$ according to the orientation. Denote by $\mathcal{M}(\mathcal{U};x)$ the longest path starting at x one traveled before meeting either x or

an ascending crossing, that is, a crossing such that one meets its underpassing strand first. The path $\mathcal{M}(\mathcal{U};x)$ is called a maximal descending path on $\mathcal{U}$ starting at x.

One defines a maximal ascending path of $\mathcal{U}$ starting at x similarly.

Following [2], we construct two special classes of resolving trees, which we call X-*coherent* and Y-*coherent*. First, we describe a class of resolving trees, referred to as *descending* ones.

Let $\mathcal{D}$ be a link diagram. Let us describe a descending resolving tree $\mathcal{T}$ of $\mathcal{D}$. The construction of the tree consists of several phases. One starts with the one vertex tree $\mathcal{T}_0$. At the end of the kth phase, one obtains a rooted subtree $\mathcal{T}_k$ of $\mathcal{T}$. The resulting subtrees satisfy

$$\{\mathcal{D}\} = \mathcal{T}_0 \subset \mathcal{T}_1 \subset \ldots \subset \mathcal{T}_m = \mathcal{T}.$$

Thus, one obtains each of the trees from the previous one by extensions shown in Figure 9.

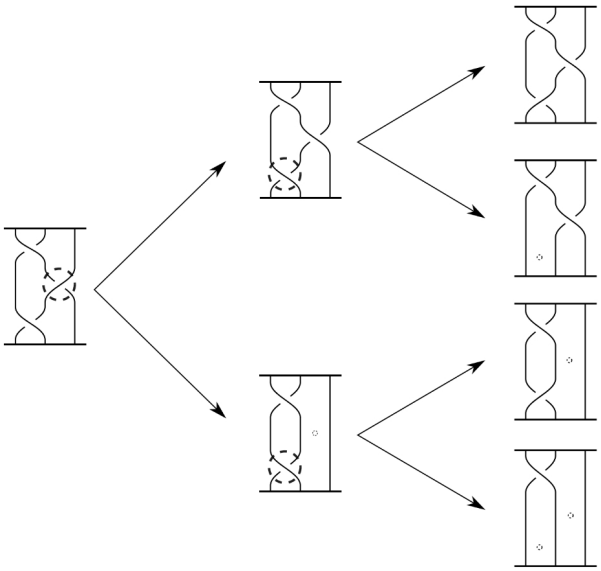

FIGURE 10. An example of a descending resolving tree. For each vertex of the tree, the base point is the input of another leftmost strand.

In the first phase, one chooses an arbitrary base point x_1 on $\mathcal{D}$. One finds the maximal descending path $\mathcal{M}(\mathcal{D};x_1)$ on $\mathcal{D}$ starting at x_1. If $\mathcal{M}(\mathcal{D};x_1)$ is closed, that is, $\mathcal{M}(\mathcal{D};x_1)$ is the whole link component of $\mathcal{D}$ containing x_1, the phase ends. Assume $\mathcal{M}(\mathcal{D};x_1)$ is not closed. In this case, one extends the current tree at a crossing of $\mathcal{D}$ that is the end of the path $\mathcal{M}(\mathcal{D};x_1)$, see Figure 9. At this moment, the tree $\mathcal{T}_1$ consists of three vertices: a parent $\mathcal{D}$ and its children $\mathcal{D}'$ and $\mathcal{D}''$. Then one finds the maximal descending path $\mathcal{M}(\mathcal{D}';x_1)$ on $\mathcal{D}'$ starting at x_1. If $\mathcal{M}(\mathcal{D}';x_1)$ is not closed, one extends the current tree $\mathcal{T}_1$ similarly by adding children of $\mathcal{D}'$. One repeats the same procedure for all leaf vertices $\mathcal{U}$ of the current tree $\mathcal{T}_1$. At the end of the first phase, for each leaf vertex $\mathcal{U}$ of $\mathcal{T}_1$, the maximal descending path $\mathcal{M}(\mathcal{U};x_1)$ on $\mathcal{U}$ starting at x_1 is closed. In this case, $\mathcal{M}(\mathcal{U};x_1)$ is the link component of $\mathcal{U}$ containing x_1. If each leaf vertex $\mathcal{U}$ of $\mathcal{T}_1$ is a knot diagram, the construction of $\mathcal{T}$ ends. Otherwise, one moves to the next phase.

In the second phase, one extends $\mathcal{T}_1$ as follows. For each leaf vertex $\mathcal{V}$ of $\mathcal{T}_1$, one chooses an arbitrary base point x_2 on a link component of $\mathcal{V}$ distinct from that of containing x_1. Note that the point x_2 depends on $\mathcal{V}$. One finds the maximal descending path $\mathcal{M}(\mathcal{V};x_2)$ on $\mathcal{U}$ starting at x_2. If $\mathcal{M}(\mathcal{V};x_2)$ is not closed, one extends the current tree at a crossing of $\mathcal{V}$ that is the

end of the path $\mathcal{M}(\mathcal{V}; x_2)$. One continues similarly. The second phase continues until for each leaf vertex $\mathcal{V}$ of the current tree $\mathcal{T}_2$, the path $\mathcal{M}(\mathcal{V}; x_2)$ is closed. In this case, $\mathcal{M}(\mathcal{V}; x_2)$ is the link component of $\mathcal{V}$ containing x_2.

One repeats the same procedure until all leaf vertices of the current tree are descending diagrams. Since any descending diagram represents an unlink, the resulting tree $\mathcal{T}$ is a resolving tree.

By varying the base points on the leaf vertices of $\mathcal{T}_0, \mathcal{T}_1, \ldots, \mathcal{T}_{m-1}$, one obtains a few descending resolving trees of $\mathcal{D}$. One may think of them as branching processes.

See Figure 10 for a descending resolving tree example of the Alexander closure of $\sigma_1^{-1}\sigma_2\sigma_1^{-1}$. For the sake of simplicity, the vertices are presented as braid diagrams.

The descending resolving trees introduced in [11] (see Theorem 2). Also, see the Hoste approach in [24] and Lemma 7.5.1 in [3].

We are in the position of describing X-coherent and Y-coherent resolving trees. Here and below, we assume that all link diagrams lie on the oriented plane $\mathbb{R}^2$. Thus, one may distinguish clockwise and counterclockwise Seifert circles of $\mathcal{D}$.

Let $\mathcal{D}$ be a link diagram. Let us describe an X-coherent resolving tree $\mathcal{T}$ of $\mathcal{D}$. The construction of the tree consists of several phases. One starts with the one vertex tree $\mathcal{T}_0$. At the end of the kth phase, one obtains a rooted subtree $\mathcal{T}_k$ of $\mathcal{T}$. The resulting subtrees satisfy

$$\{\mathcal{D}\} = \mathcal{T}_0 \subset \mathcal{T}_1 \subset \ldots \subset \mathcal{T}_m = \mathcal{T}.$$

Thus, one obtains each of the trees from the previous one by extensions shown in Figure 9.

Following Remark 2.2, one defines two rules called descending and ascending ones. In the descending rule, one keeps a descending crossing unchanged and branches on flipping and smoothing an ascending one. In the ascending rule, one does just the opposite, that is, keeps an ascending crossing currently visited, and branches on flipping and smoothing a descending one.

At each phase, one follows either the descending or ascending rule. By definition, one follows the descending rule if and only if the Seifert circle C containing a current base point x is clockwise.

More precisely, in the first phase, one chooses an arbitrary base point x_1 on $\mathcal{D}$. One finds the maximal descending (resp. ascending) path of $\mathcal{D}$ starting at x_1 whenever the corresponding Seifert circle is clockwise (resp. counterclockwise). If the path is not closed, one extends the current tree at a crossing of $\mathcal{D}$ that is the end of the path, see Figure 9. One repeats the same procedure for all leaf vertices $\mathcal{U}$ of the current tree $\mathcal{T}_1$. At the end of the first phase, for each leaf vertex $\mathcal{U}$ of $\mathcal{T}_1$, the maximal descending (resp. ascending) path of $\mathcal{U}$ starting at x_1 is closed. If each leaf vertex $\mathcal{U}$ of $\mathcal{T}_1$ is a knot diagram, the construction ends.

In the second phase, one extends $\mathcal{T}_1$ as follows. For each leaf vertex $\mathcal{V}$ of $\mathcal{T}_1$, one chooses an arbitrary base point x_2 on a link component of $\mathcal{V}$ distinct from that of containing x_1. Note that the point x_2 depends on $\mathcal{V}$. One finds the maximal descending (resp. ascending) path of $\mathcal{V}$ starting at x_2 whenever the corresponding Seifert circle is clockwise (resp. counterclockwise). If the path is not closed, one extends the current tree at a crossing of $\mathcal{V}$ that is the end of the path. One continues similarly. The second phase ends when for each leaf vertex $\mathcal{V}$ of the current tree $\mathcal{T}_2$, the maximal descending (resp. ascending) path of $\mathcal{V}$ starting at x_2 is closed.

One repeats the same procedure until for each leaf vertex $\mathcal{U}$ of the current tree, all link components of $\mathcal{U}$ are visited. This completes the construction of $\mathcal{T}$.

It is easy to see that for any leaf vertex $\mathcal{U}$ of $\mathcal{T}$, each link component of $\mathcal{U}$ is either descending or ascending. Also, the link components of $\mathcal{U}$ are stacked over each other. Thus, $\mathcal{U}$ represents an unlink. Therefore, $\mathcal{T}$ is a resolving tree.

By varying the base points on the leaf vertices of $\mathcal{T}_0, \mathcal{T}_1, \ldots, \mathcal{T}_{m-1}$, one obtains a few X-coherent resolving trees of $\mathcal{D}$.

One defines a class of Y-coherent resolving trees similarly. Namely, one follows the descending rule if and only if the Seifert circle containing a current base point is counterclockwise.

To prove Theorem 1.4, we use specific X-coherent and Y-coherent resolving trees, which we define below.

2.2. **Castle structure for link diagrams.** Following [2], we describe an additional structure for a link diagram, which is called a *castle*. The castle consists of several segments on Seifert circles, which are called *floors*, and several crossings between them, which are called *ladders*.

Let $\mathcal{D}$ be a link diagram. A Seifert circle C of $\mathcal{D}$ is said to be *innermost* if C does not bound any other Seifert circle inside it.

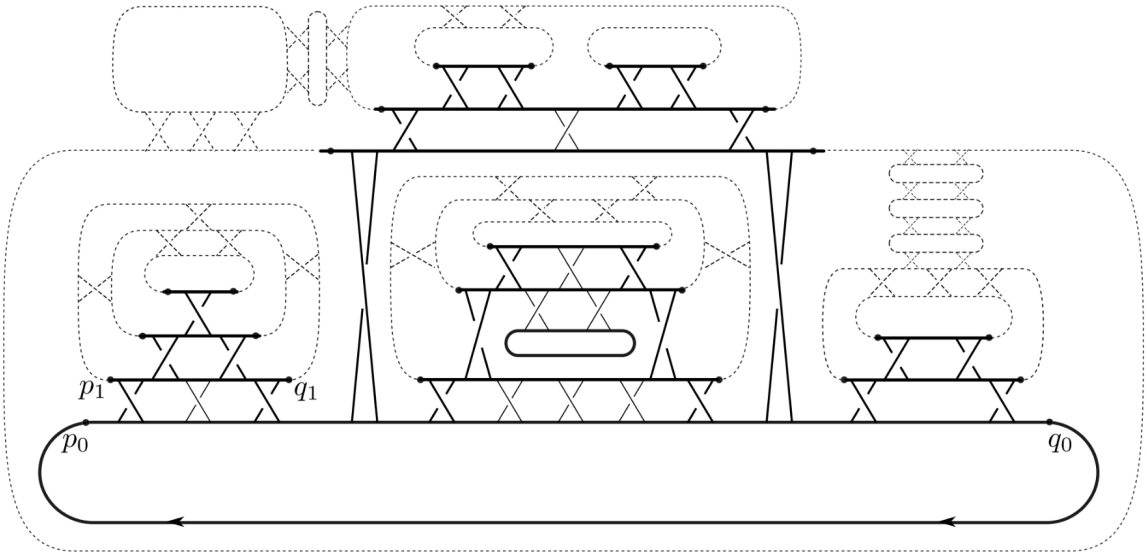

FIGURE 11. An example of a castle.

Let C be an innermost Seifert circle of $\mathcal{D}$. Choose a base point on C. If C has no adjacent crossings, the castle is empty. Assume C is adjacent to at least one crossing of $\mathcal{D}$. Starting at x and following the orientation of C, one orders the crossings adjacent to C, as shown in Figure 11. Since C is innermost, the crossings lie on the same side of C. Denote by p_0 and q_0 the ends of a segment on C that involves all of the crossings such that p_0 is the base point and q_0 is the point immediately after the last crossing adjacent to C. This segment of C is called a *floor of level* 0.

Let C' be a Seifert circle of $\mathcal{D}$ that shares common crossings with C. Let p_1 and q_1 be two points on C' immediately before the first common crossing and immediately after the last common crossing, respectively. The segment of C' between p_1 and q_1 is called a *floor of level* 1. If C shares common crossings with another Seifert circle of $\mathcal{D}$, one constructs another floor of level 1 similarly. Eventually, one constructs all floors of level 1 of the castle.

Let C' be a Seifert circle containing a floor F of level 1. If F has no common crossings with other Seifert circles of $\mathcal{D}$, then F terminates. Note that one allows C' to have adjacent crossings, not lying directly on F. Assume F has common crossings with other Seifert circles of $\mathcal{D}$. Starting at p_1 and following the orientation of C', one orders these crossings. Note that they may lie on both sides of F. Let C'' be a Seifert circle of $\mathcal{D}$ that shares common crossings with F. Let p_2 and q_2 be two points on C'' immediately before the first common crossing and immediately after the last common crossing, respectively. The segment of C'' between p_2 and q_2 is called a *floor of level* 2. If F shares common crossings with another Seifert circle of $\mathcal{D}$, one constructs another floor of level 2 adjacent to F similarly. After F is done, one moves to another floor of level 1. Eventually, one constructs all floors of level 2 of the castle.

One repeats the same procedure until one constructed all possible floors. A crossing s of $\mathcal{D}$ is called a *ladder* if s connects two floors of the castle. By definition, the resulting castle is a collection of all such floors and ladders.

It is easy to see that there may be more than one separate floor on top of any given floor. Let F_m be a top floor of level $m \geq 0$, F_{m-1} be the floor of level $m-1$ adjacent to F_m, F_{m-2} be the floor of level $m-2$ adjacent to F_{m-1}, and so on. The collection of floors $F_0, F_1, \ldots, F_m$ and all ladders between them is called a *tower* of the castle.

Remark 2.3. A castle has a unique floor of level 0 and several floors of higher levels. It is easy to see that any Seifert circle of $\mathcal{D}$ contains at most one floor of the castle. Note that there may be crossings of $\mathcal{D}$ that are not ladders of the castle and Seifert circles of $\mathcal{D}$ that do not contain floors of the castle. The castle is uniquely determined by the starting innermost Seifert circle C and a base point on it.

A castle is said to be *trapped* if there are two adjacent floors F_1 and F_2 and two adjacent ladders s_1 and s_2 connecting F_1 and F_2 such that the interior of the disk bounded by s_1, s_2, F_1, and F_2 contains a floor of the castle. In this case, the disk is called a *trap*. Otherwise, the castle is said to be *free*.

A castle shown in Figure 11 is trapped. Namely, there are two traps. Roughly speaking, a castle without trapped Seifert circles consists of several braid diagrams.

Let (C, x) be a pair consisting of an innermost Seifert circle C of $\mathcal{D}$ and a base point x on C. The pair (C, x) is said to be *appropriate* if the corresponding castle is free. Note that for a given link diagram, there may be several distinct appropriate pairs.

In [2] (see Lemma 4.3), the authors proved that any link diagram $\mathcal{D}$, there exists an innermost Seifert circle C of $\mathcal{D}$ and a base point x on it such that (C, x) is appropriate. By using the same argument, we prove the following result.

Let $(\mathcal{C}, \mathcal{A}, \|\cdot\|)$ be a system of weighted circles and π be a braid placement. Let $\mathcal{D}$ be the link diagram determined by π.

Lemma 2.4. There exists an appropriate pair (C, x) of $\mathcal{D}$ such that for all $\alpha \in \mathcal{A}$, if x lies on the braid diagram corresponding to $\pi(\alpha)$, then x is an input of a strand of $\pi(\alpha)$.

Proof. Let (C, x) be a pair consisting of an innermost Seifert circle C of $\mathcal{D}$ and a base point x on C such that for all $\alpha \in \mathcal{A}$, if x lies on the braid diagram corresponding to $\pi(\alpha)$, then x is an input of a strand of $\pi(\alpha)$. Assume that the corresponding castle K is trapped. Let F_1 and F_2 be the boundary floors of the corresponding trap B. By the definition, B contains a floor of the castle K. Let C_1 be a Seifert circle of $\mathcal{D}$ lying in the trap B and containing a floor of K such that C_1 shares a common crossing with either F_1 or F_2. Let C_2 be an arbitrary innermost Seifert circle of $\mathcal{D}$ bounded by C_1. Arcs $\alpha \in \mathcal{A}$ intersecting C_2 divide C_2 into segments. Let y

be a point on any of these segments. It is easy to see that for all $\alpha \in \mathcal{A}$, if the point y lies on the braid diagram corresponding to $\pi(\alpha)$, then y is an input of a strand of $\pi(\alpha)$.

Without loss of generality, C_1 shares common crossings with F_1. It is easy to check that the graph $\Gamma(\mathcal{D})$ is bipartite. Therefore, C_1 shares no crossings with F_2. It follows that the castle M corresponding to (C_2, y) has no floors intersecting F_2. Therefore, the intersection of M and the complement of B lies within the towers of K containing F_1.

If (C_2, y) is not appropriate, one repeats the same procedure as above. By using the argument above, it is not hard to show that the process ends after finitely many steps. The lemma is proved. □

2.3. **Proof of Theorem 1.4.** Let $\mathcal{D}$ be a link diagram. Let E (resp. e) be the highest (resp. the lowest) a-degree of the skein polynomial $\mathcal{P}(\mathcal{D}; a, z)$ of $\mathcal{D}$. We aim to prove that if $\mathcal{D}$ is $-$solid, then $E = -\omega(\mathcal{D}) + s(\mathcal{D}) - 1$. By using similar arguments, one can show that if $\mathcal{D}$ is $+$solid, then $e = -\omega(\mathcal{D}) - s(\mathcal{D}) + 1$. This will prove that the Morton–Franks–Williams inequality is sharp for any solid link diagram.

Let $(\mathcal{C}, \mathcal{A}, \|\cdot\|)$ be a system of weighted circles and π be a braid placement. Let $\mathcal{D}$ be the link diagram determined by π.

Remark 2.5. Suppose one smoothed or flipped some crossings of $\mathcal{D}$ and then deleted some link components. Let $\mathcal{D}'$ be the resulting link diagram. We construct a system of weighted circles $(\mathcal{C}', \mathcal{A}', \|\cdot\|)$ and a braid placement π' such that the link diagram determined by π' is $\mathcal{D}'$ as follows. First, for each $\alpha \in \mathcal{A}$, we smooth and flip the corresponding crossings of $\pi(\alpha)$. Second, for another link component, we remove both the corresponding parts of Seifert circles and strands of braid diagrams. If one of the braid diagrams has two strands, after removing one of them, we remove the corresponding arc from the current system of weighted circles. The resulting braid diagrams $\pi'(\alpha)$ are uniquely defined up to far commutativity. It is not hard to check that if $(\mathcal{C}, \mathcal{A}, \|\cdot\|)$ is reduced, then $(\mathcal{C}', \mathcal{A}', \|\cdot\|)$ is reduced too.

Following [2], we define a class of X-coherent resolving trees, which we call *special* X-*coherent*.

Let $\mathcal{D}$ be a link diagram. Let us describe a special X-coherent resolving tree $\mathcal{T}$ of $\mathcal{D}$. As of any X-coherent resolving tree, the construction of $\mathcal{T}$ consists of several phases. One starts with the one vertex tree $\mathcal{T}_0$. At the end of the kth phase, one obtains a rooted subtree $\mathcal{T}_k$ of $\mathcal{T}$. The resulting subtrees satisfy

$$\{\mathcal{D}\} = \mathcal{T}_0 \subset \mathcal{T}_1 \subset \ldots \subset \mathcal{T}_m = \mathcal{T}.$$

Let us describe the construction of $\mathcal{T}_1$. We take an arbitrary appropriate pair (C_1, x_1) of $\mathcal{D}$ such that for all $\alpha \in \mathcal{A}$, if x_1 lies on the braid diagram corresponding to $\pi(\alpha)$, then x_1 is an input of a strand of $\pi(\alpha)$. The latter exists due to Lemma 2.4. Let x_1 be a base point of the first phase. Then we construct $\mathcal{T}_1$ as described in the definition of X-coherent trees.

Let us describe the construction of $\mathcal{T}_2$. Let $\mathcal{U}$ be a leaf vertex of $\mathcal{T}_1$. Recall that $\mathcal{U}$ contains the base point x_1. Let $\mathrm{LC}(\mathcal{U}; x_1)$ be the link component of $\mathcal{U}$ containing x_1. Denote by $\mathcal{U} \backslash \mathrm{LC}(\mathcal{U}; x_1)$ the link diagram obtained from $\mathcal{U}$ by removing $\mathrm{LC}(\mathcal{U}; x_1)$. Let π_1 be the corresponding braid placement (see Remark 2.5 above). We take an arbitrary appropriate pair (C_2, x_2) of $\mathcal{U} \backslash \mathrm{LC}(\mathcal{U}; x_1)$ such that for all $\alpha \in \mathcal{A}$, if x_2 lies on the braid diagram corresponding to $\pi_1(\alpha)$, then x_2 is an input of a strand of $\pi_1(\alpha)$. The latter exists due to Lemma 2.4. Let x_2 be a base point of the second phase concerning $\mathcal{U}$. At this moment, we follow the same rules as above. Then we repeat the same procedure for all leaf vertices $\mathcal{U}$ of $\mathcal{T}_1$. Eventually, we construct $\mathcal{T}_2$.

Let us describe the construction of $\mathcal{T}_3$. Let $\mathcal{V}$ be a leaf vertex of $\mathcal{T}_2$. Recall that $\mathcal{V}$ contains two base points: x_1 and x_2. Let $\mathrm{LC}(\mathcal{V};x_2)$ be the link component of $\mathcal{V}$ containing x_2. Denote by $\mathcal{V}\backslash(\mathrm{LC}(\mathcal{V};x_1)\cup\mathrm{LC}(\mathcal{V};x_2))$ the link diagram obtained from $\mathcal{V}$ by removing both $\mathrm{LC}(\mathcal{V};x_1)$ and $\mathrm{LC}(\mathcal{V};x_2)$. Let π_2 be the corresponding braid placement. We take an arbitrary appropriate pair (C_3,x_3) of $\mathcal{V}\backslash(\mathrm{LC}(\mathcal{V};x_1)\cup\mathrm{LC}(\mathcal{V};x_2))$ such that for all $\alpha\in\mathcal{A}$, if x_3 lies on the braid diagram corresponding to $\pi_2(\alpha)$, then x_3 is an input of a strand of $\pi_2(\alpha)$. The latter exists due to Lemma 2.4. Let x_3 be a base point of the third phase concerning $\mathcal{V}$. At this moment, we follow the same rules as above. Then we repeat the same procedure for all leaf vertices $\mathcal{V}$ of $\mathcal{T}_2$. Eventually, we construct $\mathcal{T}_3$.

Then we proceed similarly. In the end, we obtain a special X-coherent resolving tree $\mathcal{T}$.

Recall that for a given link diagram, there may be several distinct appropriate pairs. By varying them, we obtain a few special X-coherent resolving trees of $\mathcal{D}$.

Let $\mathcal{T}$ be an arbitrary special X-coherent resolving tree of $\mathcal{D}$.

Recall that given a leaf vertex $\mathcal{U}$ of $\mathcal{T}$, $\gamma(\mathcal{U})$ denotes the number of link components in a leaf vertex $\mathcal{U}$ of $\mathcal{T}$, $t(\mathcal{U})$ denotes the number of crossings of $\mathcal{D}$ that one smoothed in obtaining $\mathcal{U}$, and $t^-(\mathcal{U})$ denotes the number of negative crossings among the smoothed ones (see Remark 2.1 above). We say that a leaf vertex $\mathcal{U}$ of $\mathcal{T}$ contributes to the highest a-degree term $a^{-\omega(\mathcal{D})+s(\mathcal{D})-1}$ if

$$\omega(\mathcal{U})-\omega(\mathcal{D})+\gamma(\mathcal{U})-1=-\omega(\mathcal{D})+s(\mathcal{D})-1.$$

We are in the position of proving Theorem 1.4. The proof is in three steps.

In the first step, we show that there exists a specific leaf vertex $\mathcal{U}^*$ of $\mathcal{T}$ contributing to the highest a-degree term $a^{-\omega(\mathcal{D})+s(\mathcal{D})-1}$ such that one smoothed all positive crossings of $\mathcal{D}$ in obtaining $\mathcal{U}^*$. In the second step, we show that if a leaf vertex $\mathcal{U}$ of $\mathcal{T}$ contributes to the highest a-degree term $a^{-\omega(\mathcal{D})+s(\mathcal{D})-1}$ of $\mathcal{P}(\mathcal{D};a,z)$, then $\gamma(\mathcal{U})=s(\mathcal{D})$, $\omega(\mathcal{U})=0$, and $t^-(\mathcal{U})\le t^-(\mathcal{U}^*)$. In the third step, we show that the previous steps imply the result.

Step 1. We start with the following observation.

Lemma 2.6. Suppose a $(-1,-1,\dots,-1)$-homogeneous braid word u represents $\Delta_{1,n}^{-1}$. Then there exist braid words of the form $u_1\sigma_1^{-1}\sigma_2^{-1}\dots\sigma_{n-1}^{-1}u_2$ and $u_3\sigma_{n-1}^{-1}\sigma_{n-2}^{-1}\dots\sigma_1^{-1}u_4$ lying in the same far commutativity class as of the braid word u such that $u_2,u_3\in\{\sigma_1^{-1},\sigma_2^{-1},\dots,\sigma_{n-2}^{-1}\}^*$ and $u_1,u_4\in\{\sigma_2^{-1},\sigma_3^{-1},\dots,\sigma_{n-1}^{-1}\}^*$.

FIGURE 12. An illustration for Lemma 2.6.

Proof. We show that by using the moves corresponding to the far commutativity relations, one may transform u into a braid word of the form $u_1\sigma_1^{-1}\sigma_2^{-1}\dots\sigma_{n-1}^{-1}u_2$. For the second braid word, the argument is similar.

First, the statement of the lemma holds for the braid word (1.4).

Second, any two $(-1,-1,\dots,-1)$-homogeneous braid words representing the same braid are related by the diagram transformations corresponding to the braid relations and the far commutativity relations (see Theorem 9.2.5 in [7]). It is easy to check that if one obtains a

braid word v_2 from v_1 via a single move corresponding to a braid relation, the assertion holds for v_1 if and only if it holds for v_2. Similar is true for a single move corresponding to a far commutativity relation. Therefore, the statement of the lemma holds for u. The lemma is proved. □

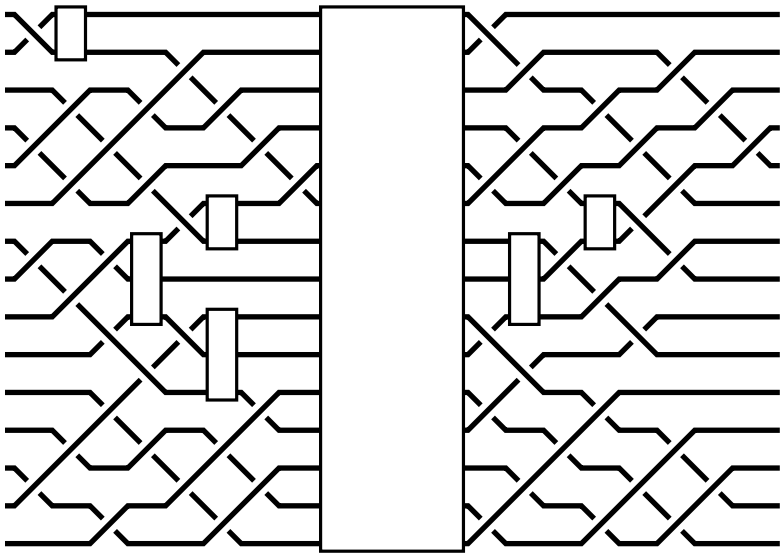

FIGURE 13. An example of a solid braid diagram. The rectangles can be filled by arbitrary braid diagrams so that the resulting one is homogeneous.

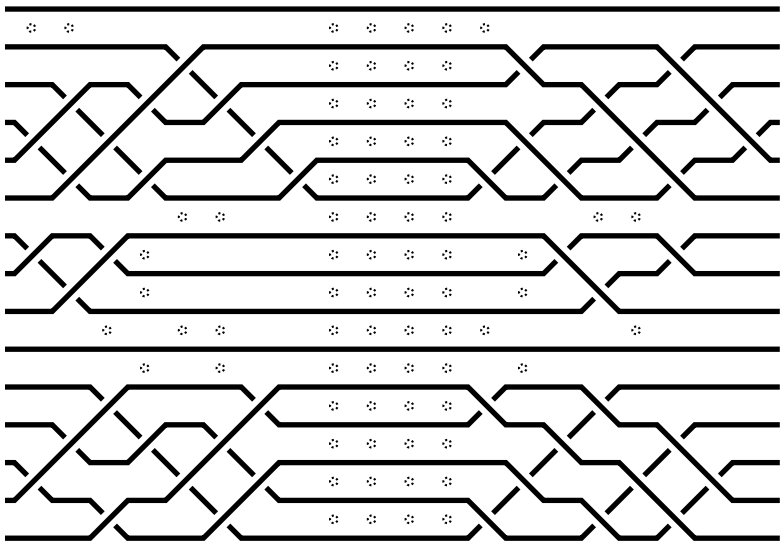

FIGURE 14. The braid diagram obtained from those in Figure 13 in the construction of $\mathcal{U}^*$.

Recall that for any leaf vertex of a resolving tree, there is a unique path from the root to the leaf. The path corresponds to a sequence of diagrams leading to the leaf vertex diagram. To prove the existence of $\mathcal{U}^*$, we construct such a path.

Let (C_1, x_1) be the appropriate pair that one used in the first phase to construct $\mathcal{T}$. Start at x_1 and move according to the orientation. Assume at the moment that C_1 intersects an

arc of the system of weighted circles. Let $\alpha \in \mathcal{A}$ be the first such arc one encountered. By the construction of (C_1, x_1), the base point x_1 is an input of a strand of $\pi(\alpha)$.

Recall that $\|\alpha\|$ denotes the number of strands in the braid diagram corresponding the braid word $\pi(\alpha)$. Given a braid diagram $\mathcal{V}$, the vertical lines containing the inputs of the strands of $\mathcal{V}$ are referred to as Seifert segments of $\mathcal{V}$.

Case 1. The first crossing one encounters is negative. This crossing has the form either σ_1^{-1} or $\sigma_{\|\alpha\|-1}^{-1}$ depending on the direction of C_1. Suppose C_1 is clockwise. Then the first crossing has the form σ_1^{-1}. Recall that in this case, one has to follow the descending rule. One has no choice but to keep the first crossing unchanged (and hence cross it). One continues traveling along the second Seifert segment of $\pi(a)$.

We assume at the moment that $i_2 > 2$. Recall that $\pi(\alpha)$ is $-$solid. One waits for a crossing of the form σ_2^{-1}. The latter exists due to Lemma 2.6. When such a crossing appears, one has no choice but to keep it unchanged. One continues traveling along the third Seifert segment of $\pi(\alpha)$ and waits for a crossing of the form σ_3^{-1}. The latter exists due to Lemma 2.6. This process continues until one crosses a crossing of the form $\sigma_{i_2-1}^{-1}$.

Let q be the last appearance of the letter $\sigma_{i_2-1}^{-1}$ in $\pi(\alpha)$ such that $\sigma_{i_2-1}^{-1}\sigma_{i_2-2}^{-1}\dots\sigma_3^{-1}\sigma_2^{-1}\sigma_1^{-1}$ is a subsequence of the suffix of $\pi(\alpha)$ that begins at q. The latter exists due to Lemma 2.6. One continues traveling along the Seifert segment i_2 of $\pi(\alpha)$. One smooths all crossings of the forms $\sigma_{i_2-1}^{-1}$ and σ_{i_2} and waits for the crossing corresponding to q. When this crossing appears, one flips it and hence moves to the Seifert segment $i_2 - 1$ of $\pi(\alpha)$.

Let q' be the last appearance of the letter $\sigma_{i_2-2}^{-1}$ in $\pi(\alpha)$ such that $\sigma_{i_2-2}^{-1}\sigma_{i_2-3}^{-1}\dots\sigma_3^{-1}\sigma_2^{-1}\sigma_1^{-1}$ is a subsequence of the suffix of $\pi(\alpha)$ that begins at q'. The latter exists due to Lemma 2.6. One continues traveling along the Seifert segment $i_2 - 1$ of $\pi(\alpha)$. One waits for the crossing corresponding to q'. When this crossing appears, one flips it and hence moves to the Seifert segment $i_2 - 2$ of $\pi(\alpha)$. This process continues until one flips a crossing of the form σ_1^{-1} and hence moves to the ending point of the first Seifert segment of $\pi(\alpha)$. The case $i_2 = 2$ is similar.

If C_1 is counterclockwise, the argument is the same after one replaces the descending algorithm by the ascending one. The first case is complete.

Case 2. The first crossing one encounters is positive. This crossing has the form either σ_1 or $\sigma_{\|\alpha\|-1}$ depending on the direction of C_1. Suppose C_1 is clockwise. Then the first crossing has the form σ_1. Recall that in this case, one has to follow the descending rule. One smooths the first crossing and continues traveling along the first Seifert segment of $\pi(\alpha)$. Repeating this process, one arrives at the end of the first Seifert segment of $\pi(\alpha)$ by smoothing all the crossings of the form σ_1.

If C_1 is counterclockwise, then one has to follow the ascending rule. One smooths all crossings of the form $\sigma_{\|\alpha\|-1}$ similarly. The second case is complete.

After the first arc α passed, one continues moving according to the orientation. If there is another arc intersecting C_1, one follows the same rules as above. Finally, one obtains a leaf vertex $\mathcal{U}_1^*$ of $\mathcal{T}_1$. Recall that to obtain the second base point of $\mathcal{U}_1^*$, one removes the link component $\mathrm{LC}(\mathcal{U}_1^*; x_1)$ of $\mathcal{U}_1^*$ containing x_1 from consideration. Let $\mathcal{U}_1^* \backslash \mathrm{LC}(\mathcal{U}_1^*; x_1)$ be the resulting link diagram. Let π_1 be the corresponding braid placement. By using Lemma 2.6, it is easy to see that π_1 is $-$solid. Thus, one can repeat the same process until the construction of $\mathcal{U}^*$ ends.

Note that in the construction of an X-coherent resolving tree, one visits each crossing of $\mathcal{D}$ exactly twice (and hence at least once). By the definition of $\mathcal{U}^*$, one smoothed all positive

crossings one encountered. Therefore, one smoothed all positive crossings of $\mathcal{D}$ in obtaining $\mathcal{U}^*$. The first step is complete.

Step 2. Let $\mathcal{U}$ be a leaf vertex of $\mathcal{T}$. Let P be a unique path from the root of $\mathcal{T}$ to $\mathcal{U}$. Given $i \in \{1, 2, \dots, \gamma(\mathcal{U})\}$, let $\mathcal{U}_i$ be a unique leaf of $P \cap \mathcal{T}_i$. Let $\mathcal{U}_0 := \mathcal{D}$. Recall that $\mathcal{U}_i$ contains i base points, which we denote by $x_1, x_2, \dots, x_i$. By the construction of $\mathcal{T}$, to obtain $\mathcal{U}_i$, one smooths all crossings of $\mathcal{U}_{i-1}$ adjacent to $\mathrm{LC}(\mathcal{U}_i; x_i)$ and then flips several crossings that $\mathrm{LC}(\mathcal{U}_i; x_i)$ intersects. Let

$$\mathcal{U}^{i-1} := \mathcal{U}_{i-1} \backslash (\mathrm{LC}(\mathcal{U}_{i-1}; x_1) \cup \mathrm{LC}(\mathcal{U}_{i-1}; x_2) \cup \ldots \cup \mathrm{LC}(\mathcal{U}_{i-1}; x_{i-1}))$$

be the link diagram obtained from the diagram $\mathcal{U}_{i-1}$ by removing the link components $\mathrm{LC}(\mathcal{U}_{i-1}; x_1), \mathrm{LC}(\mathcal{U}_{i-1}; x_2), \dots, \mathrm{LC}(\mathcal{U}_{i-1}; x_{i-1})$. Let (C_i, x_i) be the appropriate pair of the diagram $\mathcal{U}^{i-1}$ that is used in the construction of $\mathcal{T}$ concerning $\mathcal{U}_i$. Let K_i be the corresponding castle. The link component $\mathrm{LC}(\mathcal{U}_i; x_i)$ of $\mathcal{U}_i$ determines a path on K_i. This path corresponds to the natural travel through $\mathcal{U}_i$ starting at x_i. During this travel, one eventually exits the castle K for the first time through the endpoint of some floor of level L_i. The following results are Lemma 5.2 and Corollary 5.3 in [2], respectively.

Lemma 2.7. If the leaf vertex $\mathcal{U}$ contributes to the highest a-degree term $a^{-\omega(\mathcal{D})+s(\mathcal{D})-1}$, then for each index $i \in \{1, 2, \dots, \gamma(\mathcal{U})\}$, one has $L_i = 0$.

Corollary 2.8. If the leaf vertex $\mathcal{U}$ contributes to the highest a-degree term $a^{-\omega(\mathcal{D})+s(\mathcal{D})-1}$, then each link component of $\mathcal{U}$ represents a simple closed curve on $\mathbb{R}^2$.

The results above imply the following property of leaf vertices of $\mathcal{T}$ contributing to the highest a-degree term.

Corollary 2.9. If the leaf vertex $\mathcal{U}$ contributes to the highest a-degree term $a^{-\omega(\mathcal{D})+s(\mathcal{D})-1}$, then $\gamma(\mathcal{U}) = s(\mathcal{D})$ and $\omega(\mathcal{U}) = 0$.

Proof. By using Lemma 2.7, we see that for each $i \in \{1, 2, \dots, \gamma(\mathcal{U})\}$, one has

$$s(\mathcal{U}^i) = s(\mathcal{U}^{i-1}) - 1.$$

Therefore, the number of link components of $\mathcal{U}$ is $s(\mathcal{D})$.

Recall that the link components of $\mathcal{U}$ are stacked over each other. Thus, the contribution of crossings between any two distinct link components of $\mathcal{U}$ to the writhe $\omega(\mathcal{U})$ is zero. By Corollary 2.8, no link component of $\mathcal{U}$ cross itself. Therefore, $\omega(\mathcal{U}) = 0$. The corollary is proved. □

Suppose $\mathcal{U}$ contributes to the highest a-degree term $a^{-\omega(\mathcal{D})+s(\mathcal{D})-1}$. We need the following auxiliary result.

Lemma 2.10. Suppose $(\mathcal{C}, \mathcal{A}, \|\cdot\|)$ is reduced. Let $i \in \{1, 2, \dots, \gamma(\mathcal{U})\}$ and $\alpha \in \mathcal{A}$. Suppose the link component $\mathrm{LC}(\mathcal{U}; x_i)$ of $\mathcal{U}$ determines a strand $s(\alpha, i)$ on the braid diagram $\pi(\alpha)$. Then the index of the input of $s(\alpha, i)$ equals to the index of the output of $s(\alpha, i)$.

Proof. First, suppose $i = 1$. Let (C_1, x_1) be the appropriate pair of the diagram $\mathcal{U}^0 = \mathcal{D}$ that is used in the construction of $\mathcal{T}$ concerning $\mathcal{U}_1$. Let K_1 be the corresponding castle. Starting at x_1 and following the orientation of C_1, let us order the arcs of $\mathcal{A}$ intersecting C_1 as $\alpha_1, \alpha_2, \dots, \alpha_r$.

Let $d_1 \in \{1, 2, \dots, \|\alpha_1\|\}$ be the index of the output of $s(\alpha_1, 1)$. We aim to prove that $d_1 = 1$.

Assume the converse, that is, $d_1 > 1$. Let $p_0 = x_1$ and q_0 be the ends of the floor of level 0 of K_1, see Figure 15. Note that $p_0, q_0 \in \mathrm{LC}(\mathcal{U}; x_1)$. By Lemma 2.7, the part of $\mathrm{LC}(\mathcal{U}; x_1)$

located from p_0 to q_0 contains within the castle K_1. Let $j \in \{2, 3, \dots, r\}$ be the minimum number such that the Seifert circle C containing the second Seifert segment of $\pi(\alpha_1)$ intersects α_j. Since K_1 is free, $j = 2$. Let B be the disk bounded by C_1, C, α_1 and α_2. Since K_1 is free, B represents a topological disk region in the complement of the connected component of the system of weighted circles $(\mathcal{C}, \mathcal{A}, \|\cdot\|)$ that has precisely four distinct sides. Thus, $(\mathcal{C}, \mathcal{A}, \|\cdot\|)$ is not reduced. This contradicts the assumption of the lemma. Therefore, $d_1 = 1$.

Similar arguments show that for all $\alpha \in \{\alpha_2, \alpha_3, \dots, \alpha_r\}$, the index of the input of $s(\alpha, 1)$ equals to the index of the output of $s(\alpha, 1)$. Hence, if $\mathrm{LC}(\mathcal{U}; x_1)$ intersects an arc $\alpha \in \mathcal{A}$, then $\alpha \in \{\alpha_1, \alpha_2, \dots, \alpha_r\}$. Thus, the case $i = 1$ is complete.

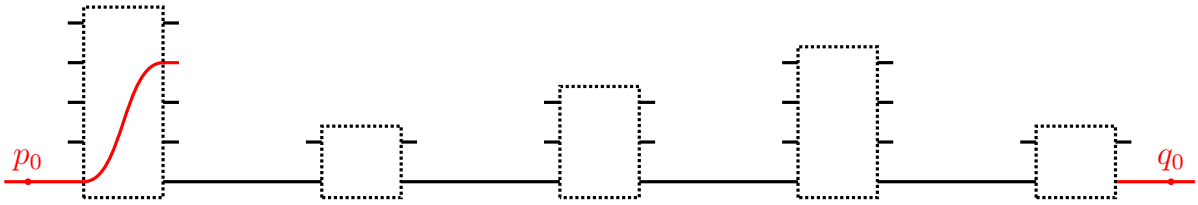

FIGURE 15. An illustration for Lemma 2.10.

Suppose $i = 2$. Let (C_2, x_2) be the appropriate pair of the diagram $\mathcal{U}^1 = \mathcal{U}_1 \backslash \mathrm{LC}(\mathcal{U}_1; x_1)$ that is used in the construction of $\mathcal{T}$ concerning $\mathcal{U}_2$. Let $(\mathcal{C}', \mathcal{A}', \|\cdot\|)$ be the corresponding system of weighted circles and π_2 be the corresponding braid placement such that the link determined by π_2 is $\mathcal{U}^1$. Since $(\mathcal{C}, \mathcal{A}, \|\cdot\|)$ is reduced, $(\mathcal{C}', \mathcal{A}', \|\cdot\|)$ is reduced too (see Remark 2.5). Therefore, one can apply the same arguments as above.

The case $i > 2$ is similar. The lemma is proved. □

We are in the position of proving the inequality $t^-(\mathcal{U}) \leq t^-(\mathcal{U}^*)$.

Let $\alpha \in \mathcal{A}$. Let $r_1, \dots, r_{\|\alpha\|-1} \in \{1, -1\}$ be such that $\pi(\alpha)$ is $(r_1, \dots, r_{\|\alpha\|-1})$-homogeneous. Let $i_1, i_2, \dots, i_m \in \{1, 2, \dots, \|\alpha\|\}$ be indexes such that $1 = i_1 < i_2 < \dots < i_m = \|\alpha\|$ and for all $k \in \{1, 2, \dots, m-1\}$, one has $r_{i_k} = r_{i_k+1} = \dots = r_{i_{k+1}-1}$ and $r_{i_{k+1}-1} \neq r_{i_{k+1}}$. By the definition of $-$solid braids, for each $k \in \{1, 2, \dots, m-1\}$ such that $r_{i_k} = -1$, the braid word obtained from $\pi(\alpha)$ by deleting all letters except $\sigma_{i_k}^{-1}, \sigma_{i_k+1}^{-1}, \dots, \sigma_{i_{k+1}-1}^{-1}$ admits a decomposition of the form $v_{k,1}v_{k,2}v_{k,3}$ such that both $v_{k,1}$ and $v_{k,3}$ represent $\Delta^{-1}_{i_k, i_{k+1}}$. See Figure 13 above.

Let $\pi_{\gamma(\mathcal{U})}$ be the braid placement corresponding to $\mathcal{U}_{\gamma(\mathcal{U})} = \mathcal{U}$. Given a braid word w, denote by $|w|$ the length of w.

Lemma 2.11. For each $k \in \{1, 2, \dots, m-1\}$ such that $r_{i_k} = -1$, one neither smoothed nor flipped at least $2|v_{k,1}|$ negative crossings of $\pi(\alpha)$ in obtaining $\pi_{\gamma(\mathcal{U})}(\alpha)$.

Proof. Without loss of generality, $r_1 = -1$. First, suppose $k = 1$.

Let $i \in \{1, 2, \dots, \gamma(\mathcal{U})\}$ be the index such that the input of the first Seifert segment of $\pi(\alpha)$ lies on $\mathrm{LC}(\mathcal{U}; x_i)$. The link component $\mathrm{LC}(\mathcal{U}; x_i)$ of $\mathcal{U}$ containing x_i determines a path P on $\pi(\alpha)$. This path corresponds to the natural travel through $\pi_{\gamma(\mathcal{U})}(\alpha)$ starting at the input of the first Seifert segment of $\pi(\alpha)$. It is easy to see that P contains crossings of $v_{1,1}$ of the form $\sigma_1^{-1}, \sigma_2^{-1}, \dots, \sigma_{i_2-1}^{-1}$ (see Lemma 2.6). Due to Lemma 2.10, the path P exits $\pi(\alpha)$ through the endpoint of the first Seifert segment of $\pi(\alpha)$. Therefore, P contains at least $i_2 - 1$ additional crossings of $\pi(\alpha)$ of the form $\sigma_{i_2-1}^{-1}, \sigma_{i_2-2}^{-1}, \dots, \sigma_1^{-1}$. Therefore, one neither smoothed nor flipped at least $2(i_2 - 1)$ negative crossings of $\pi(\alpha)$ in obtaining $\pi_{\gamma(\mathcal{U})}(\alpha)$.

For each $j \in \{1, 2, \dots, i_2 - 1\}$, we apply similar arguments concerning the link component of $\mathcal{U}$ containing the input of the index j Seifert segment of $\pi(\alpha)$. We see that one neither

smoothed nor flipped at least

$$2(i_2-1)+2(i_2-2)+\ldots+2=2i_2(i_2-1)=2|v_{1,1}|$$

negative crossings of $\pi(\alpha)$ in obtaining $\pi_{\gamma(\mathcal{U})}(\alpha)$.

For $k>1$ such that $r_{i_k}=-1$, the argument is similar. The lemma is proved. □

Denote by $t^-(\mathcal{U}^*;\alpha)$ (resp. $t^-(\mathcal{U};\alpha)$) the number of negative crossings of $\pi(\alpha)$ that one smoothed in obtaining $\mathcal{U}^*$ (resp. $\mathcal{U}$). Denote by $n(\pi(\alpha))$ the number of negative crossings of $\pi(\alpha)$. One has

$$t^-(\mathcal{U}^*;\alpha)+\sum_{\substack{k\in\{1,2,\ldots,m-1\}\\ r_{i_k}=-1}}2|v_{k,1}|=n(\pi(\alpha)), \tag{2.1}$$

see Figure 14. Lemma 2.11 implies that

$$\sum_{\substack{k\in\{1,2,\ldots,m-1\}\\ r_{i_k}=-1}}2|v_{k,1}|\leq n(\pi(\alpha))-t^-(\mathcal{U};\alpha). \tag{2.2}$$

By combining (2.1) and (2.2), one has $t^-(\mathcal{U};\alpha)\leq t^-(\mathcal{U}^*;\alpha)$. Therefore,

$$t^-(\mathcal{U})=\sum_{a\in\mathcal{A}}t^-(\mathcal{U};\alpha)\leq\sum_{\alpha\in\mathcal{A}}t^-(\mathcal{U}^*;\alpha)=t^-(\mathcal{U}^*).$$

The second step is complete.

Step 3. Let $\mathcal{V}$ be a leaf vertex of $\mathcal{T}$. Recall that the contribution of $\mathcal{V}$ to $\mathcal{P}(\mathcal{D};a,z)$ is

$$(-1)^{t^-(\mathcal{V})}z^{t(\mathcal{V})}a^{\omega(\mathcal{V})-\omega(\mathcal{D})}((a-a^{-1})z^{-1})^{\gamma(\mathcal{V})-1},$$

see Remark 2.1. Therefore, the highest a-degree term that $\mathcal{V}$ contributes to $\mathcal{P}(\mathcal{D};a,z)$ is

$$(-1)^{t^-(\mathcal{V})}z^{t(\mathcal{V})-\gamma(\mathcal{V})+1}a^{\omega(\mathcal{V})-\omega(\mathcal{D})+\gamma(\mathcal{V})-1}.$$

In [2] (see the beginning of section 5), the authors showed that

$$\omega(\mathcal{V})-\omega(\mathcal{D})+\gamma(\mathcal{V})-1\leq-\omega(\mathcal{D})+s(\mathcal{D})-1.$$

Recall that in the first step, we showed that there exits a leaf vertex $\mathcal{U}^*$ of $\mathcal{T}$ that contributes to the the highest a-degree term $a^{-\omega(\mathcal{D})+s(\mathcal{D})-1}$.

Let $\mathcal{U}$ be a leaf vertex of $\mathcal{T}$ that contributes to the the highest a-degree term $a^{-\omega(\mathcal{D})+s(\mathcal{D})-1}$. Recall that in the second step, we showed that $\gamma(\mathcal{U})=s(\mathcal{D})$, $\omega(\mathcal{U})=0$, and $t^-(\mathcal{U})\leq t^-(\mathcal{U}^*)$. It is easy to see that $\mathcal{U}$ contributes to the term

$$z^{t(\mathcal{U}^*)-s(\mathcal{D})+1}a^{-\omega(\mathcal{D})+s(\mathcal{D})-1} \tag{2.3}$$

if and only if $t(\mathcal{U})=t(\mathcal{U}^*)$.

Suppose $t(\mathcal{U})=t(\mathcal{U}^*)$. Denote by $p(\mathcal{D})$ the number of positive crossings of $\mathcal{D}$. Given a leaf vertex $\mathcal{V}$ of $\mathcal{T}$, denote by $t^+(\mathcal{V})$ the number of positive crossings of $\mathcal{D}$ that one smoothed in obtaining $\mathcal{V}$. Recall that in the first step, we showed that $t^+(\mathcal{U}^*)=p(\mathcal{D})$. One has

$$t^-(\mathcal{U}^*)=t(\mathcal{U}^*)-t^+(\mathcal{U}^*)=t(\mathcal{U})-p(\mathcal{D})\leq t(\mathcal{U})-t^+(\mathcal{U})=t^-(\mathcal{U}).$$

Hence, $t^-(\mathcal{U})=t^-(\mathcal{U}^*)$. Therefore, the contribution of $\mathcal{U}$ to the term (2.3) has the same sign $(-1)^{t^-(\mathcal{U}^*)}$ as of $\mathcal{U}^*$. Thus, the term do not cancel. This shows that

$$E=-\omega(\mathcal{D})+s(\mathcal{D})-1.$$

The third step is complete. Theorem 1.4 is proved.

3. Polynomial invariants of tangles and braids

In this section, we show that certain polynomial invariants of tangles provide lower bounds on the crossing number.

In [51], J. Conway introduced an invariant $\nabla(\mathcal{L};z)\in\mathbb{Z}[z^{\pm1}]$ of links. The latter is referred to as the *Conway polynomial*. This polynomial is a specialization of the skein polynomial. Namely, $\nabla(\mathcal{L};z)=\mathcal{P}(\mathcal{L},1,z)$. Following [40], we recall the definition of a polynomial invariant of ordered tangles similar to the Conway polynomial.

We assume that all tangle diagrams are oriented. In this section, we treat braid diagrams as tangle diagrams and treat braids as tangles.

Let $\mathcal{D}$ be a tangle diagram. A collection of m crossings of $\mathcal{D}$ is called an *m-state* of $\mathcal{D}$. A state S of $\mathcal{D}$ determines a new tangle diagram $\mathcal{R}(S)$ obtained from $\mathcal{D}$ by smoothing all crossings lying in S. Suppose $\mathcal{R}(S)$ has no closed components. Choose an order on the set of strands. One travels through $\mathcal{R}(S)$ by moving through each strand naturally. In this process, one passes a neighborhood of each smoothed crossing $c\in S$ twice. The state S is said to be *descending* if, for each $c\in S$, one enters this neighborhood first time on the overpass of $\mathcal{D}$.

Denote by H the union of inputs and outputs of all strands of $\mathcal{D}$. A bijective function

$$\tau : H \longrightarrow \{1,2,\dots,2n\}$$

is called an *ordering* of $\mathcal{D}$ if $\tau(x)$ is odd whenever x is an input. A pair consisting of a tangle diagram and its ordering τ is called a τ-ordered tangle diagram.

An ordering τ is said to be *coherent* if, for any strand of $\mathcal{D}$ with input x and output y, one has $\tau(y)=\tau(x)+1$. A state S of a τ-ordered tangle diagram is said to be *coherent* if $\mathcal{R}(S)$ contains no closed components, and the ordering of $\mathcal{R}(S)$ induced by τ is coherent.

We order the strands according to images $\tau(x)$ of their inputs $x\in H$. A coherent state S is said to be *τ-descending* if S is descending with respect to this order. Denote by $t^-(S)$ the number of negative crossings of $\mathcal{D}$ lying in S.

Let $\mathcal{D}$ be a τ-ordered tangle diagram. By $\mathcal{S}_m(\mathcal{D},\tau)$ we denote the set of all τ-descending m-states of $\mathcal{D}$. Define the *Conway polynomial* $\nabla(\mathcal{D},\tau;z)\in\mathbb{Z}[z]$ of $\mathcal{D}$ as follows:

$$\nabla(\mathcal{D},\tau;z)=\sum_{m=0}^{\infty}\left(\sum_{S\in\mathcal{S}_m(\mathcal{D},\tau)}(-1)^{t^-(S)}\right)z^m.$$

We emphasize that $\nabla(\mathcal{D},\tau;z)$ depends on the ordering τ. In [40], the author proved (see Theorem 4.6) that if two τ-ordered tangle diagrams $\mathcal{D}$ and $\mathcal{D}'$ represent the same tangle, then $\nabla(\mathcal{D},\tau;z)=\nabla(\mathcal{D}',\tau;z)$.

3.1. **Proof of Proposition 1.12.** Given a tangle diagram $\mathcal{D}$, denote by $|\mathcal{D}|$ the number of crossings of $\mathcal{D}$. The diagram $\mathcal{D}$ is said to be *minimal* if $\mathcal{D}$ has the least possible number of crossings among all diagrams representing the same tangle.

A τ-ordered tangle diagram $\mathcal{D}$ is said to be *τ-special* if $\mathcal{S}_{|\mathcal{D}|}(\mathcal{D},\tau)$ is non-empty, that is, a unique $|\mathcal{D}|$-state of $\mathcal{D}$ is τ-descending.

Lemma 3.1. Let $\mathcal{D}$ be a τ-ordered tangle diagram. One has

$$\deg\,\nabla(\mathcal{D},\tau;z)\le|\mathcal{D}|. \tag{3.1}$$

The equality holds if and only if $\mathcal{D}$ is τ-special.

Proof. First, for $m>|\mathcal{D}|$, the set $\mathcal{S}_m(\mathcal{D},\tau)$ is empty. Hence, the term of degree m in $\nabla(\mathcal{D},\tau;z)$ is zero. Therefore, $\deg\,\nabla(\mathcal{D},\tau;z)\le|\mathcal{D}|$. Second, note that $\deg\,\nabla(\mathcal{D},\tau;z)=|\mathcal{D}|$ if and only if a

term of degree $|\mathcal{D}|$ in $\nabla(\mathcal{D},\tau;z)$ is non-zero. The latter is equivalent to the fact that $\mathcal{S}_{|\mathcal{D}|}(\mathcal{D},\tau)$ is non-empty. The lemma is proved. □

Corollary 3.2. Let τ be an ordering. Assume a tangle $\mathcal{T}$ admits a τ-special diagram. A diagram $\mathcal{D}$ of $\mathcal{T}$ is minimal if and only if $\mathcal{D}$ is τ-special.

Proof. First, (3.1) implies that any τ-special diagram is minimal. Second, suppose $\mathcal{D}$ is minimal. Let $\mathcal{D}'$ be a τ-special diagram of $\mathcal{T}$. One has

$$|\mathcal{D}| = |\mathcal{D}'| = \deg\, \nabla(\mathcal{D}',\tau;z) = \deg\, \nabla(\mathcal{D},\tau;z).$$

Lemma 3.1 implies that $\mathcal{D}$ is τ-special. The corollary is proved. □

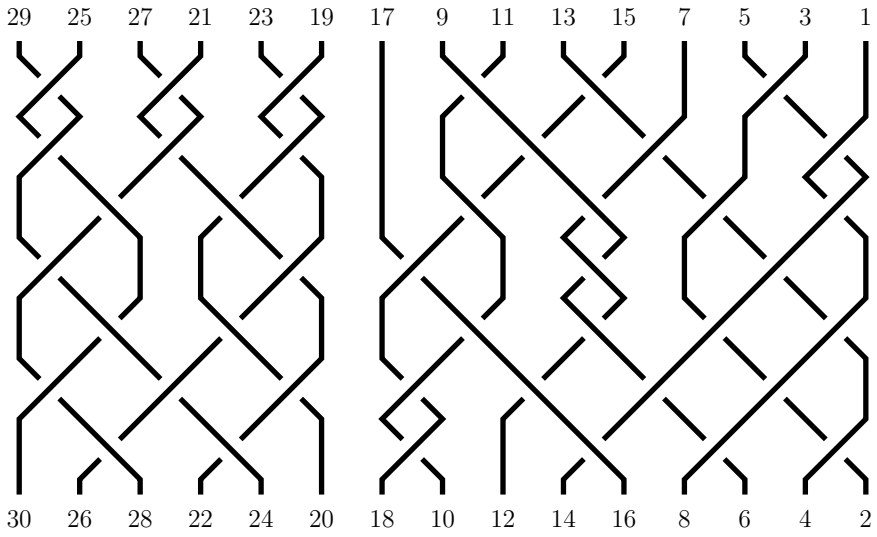

FIGURE 16. An example of a special ordering.

Let $\mathcal{D}$ be a τ-ordered tangle diagram. Suppose $\mathcal{D}$ is τ-special, that is, a unique $|\mathcal{D}|$-state S of $\mathcal{D}$ is τ-descending. Then $\mathcal{R}(S)$ has neither crossings nor closed components. Therefore, $\mathcal{D}$ is a braid diagram.

Let $\mathcal{D}$ be a τ-ordered braid diagram. It is easy to see that a unique $|\mathcal{D}|$-state S of $\mathcal{D}$ is coherent if and only if for each Seifert segment of $\mathcal{D}$ with input x and output y, one has $\tau(y) = \tau(x) + 1$. In this case, if a unique $|\mathcal{D}|$-state S of $\mathcal{D}$ is τ-descending, then $\mathcal{D}$ is homogeneous. Therefore, any special braid diagram is homogeneous.

It is easy to check that, for any homogeneous braid diagram $\mathcal{D}$, there exists at least one ordering τ such that $\mathcal{D}$ is τ-special (see Figure 16). Thus, a braid diagram $\mathcal{D}$ is special if and only if $\mathcal{D}$ is homogeneous.

Suppose a braid β admits a $(r_1, r_2, \dots, r_{n-1})$-homogeneous diagram $\mathcal{D}$. Let τ be an ordering of $\mathcal{D}$ such that $\mathcal{D}$ is τ-special. Then any τ-special diagram of β is $(r_1, r_2, \dots, r_{n-1})$-homogeneous. Therefore, Corollary 3.2 implies Proposition 1.12.

3.2. **Proof of Proposition 1.14.** Following [41], we recall the definition of a three-variable polynomial invariant $\mathcal{I} = \mathcal{I}(a,z,t)$ of braids similar to the skein polynomial.

Let $\mathcal{D}$ be a braid diagram with n strands. We enumerate by indexes $1, 2, \dots, n$ all the inputs of strands of $\mathcal{D}$ naturally from the leftmost to the rightmost, respectively.

Let $\mathcal{U}$ be a braid diagram and $k \geq 2$. A surjective function

$$C : \{1, 2, \ldots, n\} \longrightarrow \{1, 2, \ldots, k\}$$

is called a *coloring* of $\mathcal{U}$ with k colors. Roughly speaking, one paints each strand s of $\mathcal{U}$ in color $C(i(s))$, where $i(s)$ is the index of the input of s. A pair consisting of a braid diagram and its coloring of strands C is called a C-colored braid diagram.

Let $\mathcal{D}$ be a braid diagram. Given $m \geq 0$ and $k \geq 2$, denote by $[\mathcal{D}, m, k]$ the set of all pairs (S, C) consisting of an m-state S of $\mathcal{D}$ and a coloring C of $\mathcal{R}(S)$ with k colors such that

(1) any two strands of $\mathcal{R}(S)$ lying in the same link component of the Alexander closure of $\mathcal{R}(S)$ have the same color;
(2) for any positive (resp. negative) crossing $c \in S$ connecting two strands s_1 (the left one) and s_2 (the right one) of $\mathcal{R}(S)$, the color of s_1 is strictly more (reps. less) than that of s_2.

Given $(S, C) \in [\mathcal{D}, m, k]$, denote by $\mathcal{R}(S)_i$ the braid diagram consisting of all strands of $\mathcal{R}(S)$ colored by i. Given a braid diagram $\mathcal{U}$, denote by $\overline{\mathcal{U}}$ the Alexander closure of $\mathcal{U}$.

Define a Laurent polynomial $\mathcal{I}(\mathcal{D}; a, z, t) \in \mathbb{Z}[a^{\pm 1}, z^{\pm 1}, t]$ as follows. Let

$$\mathcal{I}_k(\mathcal{D}; a, z) = \sum_{m=0}^{\infty} \left(\sum_{(S,C) \in [\mathcal{D}, m, k]} (-1)^{t^-(S)} \; a^{\omega(\mathcal{R}(S))} \; \prod_{i=1}^{k} \mathcal{P}(\overline{\mathcal{R}(S)_i}; a, z) \right) z^m$$

and $\mathcal{I}(\mathcal{D}; a, z, t) = \sum_{k=2}^{\infty} \mathcal{I}_k(\mathcal{D}; a, z) t^k$. In [41], the author proved (see Theorem 1) that if two braid diagrams $\mathcal{D}$ and $\mathcal{D}'$ represent conjugate elements of $\mathcal{B}_n$, then $\mathcal{I}(\mathcal{D}; a, z, t) = \mathcal{I}(\mathcal{D}'; a, z, t)$.

Note that for any $(S, C) \in [\mathcal{D}, m, n]$ and for any $i \in \{1, 2, \ldots, n\}$, the diagram $\mathcal{R}(S)_i$ has precisely one strand. It follows that $\mathcal{I}_n(\mathcal{D}; a, z) \in \mathbb{Z}[z]$.

Lemma 3.3. Let $\mathcal{D}$ be a braid diagram with n strands. One has

$$\deg \mathcal{I}_n(\mathcal{D}; a, z) \leq |\mathcal{D}|.$$

The equality holds if and only if $\mathcal{D}$ is homogeneous.

Proof. First, for $m > |\mathcal{D}|$, the set $[\mathcal{D}, m, n]$ is empty, thus, a term of degree m in $\mathcal{I}_n(\mathcal{D}; a, z)$ is zero. Therefore, $\deg \mathcal{I}_n(\mathcal{D}; a, z) \leq |\mathcal{D}|$. Second, note that

$$\mathcal{I}_n(\mathcal{D}; a, z) = \sum_{m=0}^{|\mathcal{D}|} \left(\sum_{(S,C) \in [\mathcal{D}, m, n]} (-1)^{t^-(S)} \right) z^m,$$

thus, the highest z-degree term of $\mathcal{I}_n(\mathcal{D}; a, z)$ is

$$(-1)^{t^-(\mathcal{D})} \cdot \#[\mathcal{D}, |\mathcal{D}|, n] \cdot z^{|\mathcal{D}|}.$$

Therefore, $\deg \mathcal{I}_n(\mathcal{D}; a, z) = |\mathcal{D}|$ if and only if $[\mathcal{D}, |\mathcal{D}|, n]$ is non-empty. It is easy to see that if $\mathcal{D}$ is not homogeneous, then $[\mathcal{D}, |\mathcal{D}|, n]$ is empty. By using arguments similar to that of proving Proposition 1.12, one can show that if $\mathcal{D}$ is homogeneous, then $[\mathcal{D}, |\mathcal{D}|, n]$ is non-empty. The lemma is proved. □

Lemma 3.3 and invariance of $\mathcal{I}$ under conjugacy imply Proposition 1.14.

4. Discussion

In this section, we describe a relation between geometric group theory and knot theory.

In geometric group theory, braid words corresponding to minimal braid diagrams are referred to as *geodesic words* (with respect to the standard Artin generators). The origin of the present thesis is to study the language of geodesics for the braid groups.

There exists an explicit description of all geodesic words in $\mathcal{B}_3$ (see [42, 43]). The same is true for minimal conjugacy length words in $\mathcal{B}_3$ (see Theorem 6.1 in [46]). The language of geodesic words in $\mathcal{B}_3$ is regular and consists of 27 different cone types. It is an intriguing open problem whether the language of geodesics for $\mathcal{B}_n$ is regular for some $n \geq 4$, see [44]. Note that in [45], the authors proved that the language of geodesic words in $\mathcal{B}_n$ with respect to the generating set of simple divisors of the Garside element is regular.

A problem due to J. Stallings (see Problem 1.8 in [19]) asks whether geodesic braid words are closed under end extension (replacing a final letter s by s^n for $n \geq 2$). We present natural generalizations of this conjecture.

Conjecture 4.1. Let w, u, v be braid words in $\mathcal{B}_n$ and $s \in \{\sigma_1, \dots, \sigma_{n-1}, \sigma_1^{-1}, \dots, \sigma_{n-1}^{-1}\}$.

(1) If ws is geodesic, then wss is geodesic.
(2) If usv is geodesic, then $ussv$ is geodesic.
(3) If ws is of minimal conjugacy length, then wss is of minimal conjugacy length.

For $n = 2$, the conjecture holds. For $n = 3$, we see that the conjecture holds because of an explicit description of both geodesic and minimal conjugacy length words in $\mathcal{B}_3$. The third part of Conjecture 4.1 is also known as Question 6.1 in [46]. Propositions 1.12 and 1.14 imply the following result.

Corollary 4.2. Conjecture 4.1 holds for all homogeneous braid words.

There is a natural analog of Conjecture 4.1 for minimal link diagrams. The link diagram transformation, similar to the extension described in Conjecture 4.1, is referred to as the *doubling of a crossing*.

Conjecture 4.3. Let $\mathcal{D}$ be an oriented link diagram. Let $\mathcal{D}'$ be a diagram obtained from $\mathcal{D}$ by the doubling of a crossing. If $\mathcal{D}$ is minimal, then $\mathcal{D}'$ is minimal too.

It is easy to check that Conjecture 4.3 holds for both all adequate and all GMM diagrams. Corollary 1.6 implies the following result.

Corollary 4.4. Conjecture 4.3 holds for all solid homogeneous diagrams.

Denote by $\Gamma_n(m)$ the number of all braids β with n strands such that the crossing number of β is m. The limit

$$v(\mathcal{B}_n) := \lim_{m\to\infty} \frac{\log \Gamma_n(m)}{m}$$

is referred to as the *growth rate* and the *logarithmic volume* of the braid group $\mathcal{B}_n$. The computations show that $v(\mathcal{B}_3) = \log 2$.

One can define the growth rate for any group with a given finite generating set similarly (see Definition 7 in [47]).

In [47] (see Theorem 1), the authors calculated the growth rate for a class of groups

$$\mathcal{LF}_n = \langle a_1, \dots, a_{n-1} \mid a_i a_j = a_j a_i,\ |i-j| \geq 2 \rangle,$$

referred to as *locally free groups*. The latter are right–angled Artin groups. In particular, the authors showed that the growth rate of $\mathcal{LF}_n$ converges to $\log 7$ as n tends to infinity. By using this, they showed that

$$\log \sqrt{7} \leq \lim_{n\to\infty} v(\mathcal{B}_n) \leq \log 7,$$

see Theorem 10 in [47]. Similarly, they studied the growth rate of monoids with a given finite generating set. In particular, they calculated the growth rate for an analogous class of monoids $\mathcal{LF}_n^+$, referred to as *locally free monoids*. Also, the authors showed that the growth rate of $\mathcal{LF}_n^+$ converges to $\log 4$ as n tends to infinity. By using this, below, we show how to obtain a more accurate lower bound on the limit

$$\lim_{n\to\infty} v(\mathcal{B}_n).$$

At the end of the 19th century, P. G. Tait made three conjectures, referred to as the *Tait conjectures*, concerning alternating knots and links (see an expository note [53]):

(1) any reduced alternating diagram is minimal;
(2) any two reduced alternating diagrams representing the same link have the same writhe;
(3) any two reduced alternating diagrams representing the same link are related through a sequence of diagram transformations, referred to as *flypes* (see Figure 17).

All the Tait conjectures hold. The first Tait conjecture was discussed in the introduction of the present thesis. The second Tait conjecture follows from the third one. In [52] (see Main Theorem), W. Menasco and M. Thistlethwaite proved the third Tait conjecture, referred to as the *Tait flyping conjecture*. The latter provides a classification of alternating links.

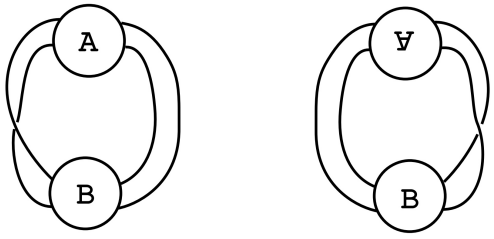

FIGURE 17. Flypes.

By using the classification of alternating knots, in [54], the authors showed that the number of knots grows at least exponentially as a function of the crossing number. We apply the same idea for braids.

Let $\mathcal{AB}_n$ be the submonoid of $\mathcal{B}_n$ generated by the set

$$\left\{\sigma_1, \sigma_2^{-1}, \sigma_3, \ldots, \sigma_{n-1}^{(-1)^n}\right\}.$$

This monoid is referred to as the *monoid of alternating braids*. By using the classification theorem for alternating links and the Alexander closure construction, it is not hard to show that the map from $\mathcal{AB}_n$ to $\mathcal{LF}_n^+$ given on generators by

$$\sigma_i^{(-1)^{i+1}} \longmapsto a_i$$

is a monoid isomorphism. Thus, the growth rate of $\mathcal{AB}_n$ is equal to that of $\mathcal{LF}_n^+$. Therefore,

$$\log 4 \leq \lim_{n\to\infty} v(\mathcal{B}_n).$$

References

[1] P. Liu, Y. Diao, G. Hetyei, *The Homfly polynomial of links in closed braid form*, Discrete Mathematics, Volume 342, Issue 1, 2019, Pages 190-200, ISSN 0012-365X, https://doi.org/10.1016/j.disc.2018.09.027.

[2] Y. Diao, G. Hetyei, P. Liu, *The braid index of reduced alternating links*, Math. Proc. Cambridge Philos. Soc. 2019: https://doi.org/10.1017/S0305004118000907.

[3] P. R. Cromwell, *Knots and Links*, Cambridge University Press, 2004.

[4] G. Burde, H. Zieschang, *Knots*, 2nd ed. de Gruyter Stud. Math. 5. Berlin: de Gruyter, 2003.

[5] M. Lackenby, *Elementary knot theory*, in Lectures on Geometry, Clay Lect. Notes, pages 29–64. Oxford Univ. Press, Oxford, 2017.

[6] W. B. R. Lickorish, *An introduction to knot theory*, Graduate Texts in Mathematics, vol. 175, Springer-Verlag, New York, 1997. MR 1472978.

[7] D. B. A. Epstein, J. W. Cannon, D. F. Holt, S. V. F. Levy, M. S. Paterson, W. P. Thurston, *Word processing in groups*, Jones and Bartlett Publishers, Boston, MA, 1992.

[8] D. Rolfsen, *Knots and links*, AMS Chelsea Publishing, 2003.

[9] C. C. Adams, *The Knot Book: An Elementary Introduction to the Mathematical Theory of Knots*, New York: W. H. Freeman and Company, 1994.

[10] J. Hoste, M. Thistlethwaite, *KnotScape*, a knot polynomial calculation and table access program, available at http://www.math.utk.edu/~morwen.

[11] P. R. Cromwell, *Homogeneous links*, Journal of the London Mathematical Society, 2(3):535–552, 1989.

[12] P. M. G. Manchòn, *Homogeneous links and the Seifert matrix*, Pacific J. Math., 255(2):373–392, 2012.

[13] M. Ozawa, *Essential state surfaces for knots and links*, J. Aust. Math. Soc. 91 (2011) 391–404 MR2900614.

[14] M. Ozawa, *Closed incompressible surfaces in the complements of positive knots*, Comment. Math. Helv., 77: 235–243 (2002).

[15] P. R. Cromwell, *Positive braids are visually prime*, Proc. London Math. Soc. (3) 67 (1993), no. 2, 384–424.

[16] W. Menasco, *Closed incompressible surfaces in alternating knot and link complements*, Topology 23 (1984) 37-44.

[17] T. Abe, K. Tagami, *Characterization of positive links and the s-invariant for links*, Canad. J. Math. 69 (2017), 1201-1218.

[18] D. Futer, E. Kalfagianni, J. Purcell, *Guts of surfaces and the colored Jones polynomial*, Lecture Notes in Mathematics, vol. 2069, Springer, Heidelberg, 2013. MR3024600.

[19] R. Kirby, *Problems in low-dimensional topology*, In Geometric Topology (Athens, GA, 1993), 35–473. AMS/IP Stud. Adv. Math. 2(2). Providence, RI: American Mathematical Society, 1997.

[20] M. Lackenby, *The crossing number of composite knots*, J. Topol. 2, no. 4 (2009): 747–68.

[21] Y. Diao, *The additivity of the crossing number*, J Knot Theory Ramif 13, 7 (2004), 857–866.

[22] H. Gruber, *Estimates for the minimal crossing number*, preprint, 2003.

[23] A. V. Malyutin, *On the question of genericity of hyperbolic knots*, Int. Math. Res. Not. (2018). https://doi.org/10.1093/imrn/rny220.

[24] P. Freyd, D. Yetter, J. Hoste, W. Lickorish, K. Millett, A. Ocneanu, *A new polynomial invariant of knots and links*, Bull. Amer. Math. Soc. (N.S.) 12 (1985) 239–246.

[25] J. Przytycki, P. Traczyk, *Conway algebras and Skein equivalence of links*, Proc. Am. Math. Soc. 100 (1987), 744–748.

[26] A. Stoimenow, *On the crossing number of positive knots and braids and braid index criteria of Jones and Morton–Williams–Franks*, Trans. Amer. Math. Soc. 354(10) (2002), 3927–3954.

[27] A. Stoimenow, *On the definition of graph index*, J. Aust. Math. Soc. 94 (2013), 417–429.

[28] K. Murasugi, *On the braid index of alternating links*, Trans. Amer. Math. Soc. 326 (1) (1991), 237–260.

[29] H. R. Morton, *Seifert circles and knot polynomials*, Math. Proc. Cambridge Philos. Soc., 99(1):107–109, 1986.

[30] J. Franks, R. F. Williams, *Braids and the Jones polynomial*, Trans. Amer. Math. Soc., 303(1):97–108, 1987.

[31] J. Gonzàlez-Meneses, P. M. G. Manchòn, *Closures of positive braids and the Morton–Franks–Williams inequality*, Topology and its Applications, Volume 174, 2014, Pages 14-24, ISSN 0166-8641, https://doi.org/10.1016/j.topol.2014.06.008.

[32] T. Kalman, *Meridian twisting of closed braids and the Homfly polynomial*, Mathematical Proceedings of the Cambridge Philosophical Society, 146(3), 649-660. doi:10.1017/S0305004108002016.

[33] T. Nakamura, *Notes on the braid index of closed positive braids*, Topology Appl. 2004, 135: 13–31.
[34] P. Feller, D. Krcatovich, *On cobordisms between knots, braid index, and the upsilon-invariant*, Math. Ann. 369 (2017), no. 1-2, 301–329. MR 3694648, https://doi.org/10.1007/s00208-017-1519-1.
[35] L. Kauffman, *State models and the Jones polynomial*, Topology 26(3) (1987), 395–407.
[36] M. Thistlethwaite, *A Spanning Tree Expansion of the Jones Polynomial*, Topology 26(3) (1987), 297–309.
[37] K. Murasugi, *The Jones Polynomial and Classical Conjectures in Knot Theory*, Topology 26 (1987): 187-194.
[38] M. B. Thistlethwaite, *On the Kauffman polynomial of an adequate link*, Invent. Math. 93, no. 2 (1988): 285–96.
[39] W. B. R. Lickorish, M. B. Thistlethwaite, *Some links with nontrivial polynomials and their crossing-numbers*, Comment. Math. Helv., 63(1), 1988, 527-539.
[40] M. Polyak, *Alexander–Conway invariants of tangles*, preprint, 2010.
[41] M. Brandenbursky, *Coloring link diagrams and Conway–type polynomial of braids*, Topology and its Applications, Volume 161, 2014, Pages 141-158, ISSN 0166-8641.
[42] L. Sabalka, *Geodesics in the braid group on three strands*, Group theory, statistics, and cryptography, 133–150, Contemp. Math., 360, Amer. Math. Soc., Providence, RI, 2004.
[43] M. Berger, *Minimum crossing numbers for 3–braids*, J. Phys. A 27 (1994), no. 18, 6205-6213.
[44] J. Mairesse, F. Mathéus, *Growth series for Artin groups of dihedral type*, Internat. J. Algebra Comput. 16 (2006), 1087–1107.
[45] R. Charney, J. Meier, *The language of geodesics for Garside groups*, Math. Zeitschrift 248 (2004), 495–509.
[46] A. Stoimenow, *Non-triviality of the Jones polynomial and the crossing numbers of amphicheiral knots*, preprint, 2007.
[47] A. M. Vershik, S. Nechaev, R. Bikbov, *Statistical properties of locally free groups with applications to braid groups and growth of random heaps*, Commun. Math. Phys. 212 (2000), 469–501.
[48] H. Chapman, *On the Structure and Scarcity of Alternating Knots*, preprint, 2018.
[49] S. Yamada, *The minimal number of Seifert circles equals the braid index of link*, Invent. Math. 891 (1987), 347–356.
[50] J. Stallings, *Constructions of fibred knots and links*, Algebraic and geometric topology (Proc. Sympos. Pure Math., XXXII, Amer. Math. Soc.), 2:55–60, 1978.
[51] J. Conway, *An enumeration of knots and links*, in: J. Leech (Ed.), Computational Problems in Abstract Algebra, Pergamon Press, 1969, pp. 329–358.
[52] W. Menasco, M. Thistlethwaite, *A classification of alternating links*, Ann. of Math. 138 (1993) 113–171.
[53] W. W. Menasco, *Alternating Knots*, preprint, 2019.
[54] C. Ernst, D. W. Sumners, *The growth of the number of prime knots*, Math. Proc. Cambridge Philos. Soc. 102 (1987), 303–315.

The author was supported by Pavel Solikov.